STANFORD RESEARCH INSTITUTE
Menlo Park, California 94025 · U.S.A.

Final Report *June 30, 1972*

INVESTIGATION OF LOW-VELOCITY DETONATION PHENOMENA IN LIQUID PROPELLANTS, FUELS, AND EXPLOSIVES

By: D. C. WOOTEN, M COWPERTHWAITE, and D. C. ERLICH

Prepared for:

DIRECTOR OF AEROMECHANICS AND ENERGETICS
AIR FORCE OFFICE OF SCIENTIFIC RESEARCH
ARLINGTON, VIRGINIA 22209
Attention: NAE

CONTRACT F44620-69-C-0079

SRI Project SCU-7771

Approved by:

G R ABRAHAMSON, *Director*
Poulter Laboratory

C J COOK, *Executive Director*
Physical Sciences Division

UNCLASSIFIED

Security Classification

DOCUMENT CONTROL DATA - R & D

(Security classification of title, body of abstract and indexing annotation must be entered when the overall report is classified)

1. ORIGINATING ACTIVITY (Corporate author)
STANFORD RESEARCH INSTITUTE
MENLO PARK, CALIFORNIA 94025

2a. REPORT SECURITY CLASSIFICATION
UNCLASSIFIED

2b. GROUP

3. REPORT TITLE

INVESTIGATION OF LOW-VELOCITY DETONATION PHENOMENA IN LIQUID PROPELLANTS, FUELS, AND EXPLOSIVES

4. DESCRIPTIVE NOTES (Type of report and inclusive dates)
Scientific Final

5. AUTHOR(S) (First name, middle initial, last name)

DAVID C WOOTEN MICHAEL COWPERTHWAITE DAVID C ERLICH

6. REPORT DATE	7a. TOTAL NO. OF PAGES	7b. NO. OF REFS
30 June 1972	116	88

8a. CONTRACT OR GRANT NO	9a. ORIGINATOR'S REPORT NUMBER(S)
F44620-69-C-0079	
b. PROJECT NO. 9711-01	SRI Project SCU-7771
c. 61102F	9b. OTHER REPORT NO(S) (Any other numbers that may be assigned this report) AFOSR - TR - 72 - 1716
d. 681308	

10. DISTRIBUTION STATEMENT

Approved for public release; distribution unlimited.

11. SUPPLEMENTARY NOTES	12. SPONSORING MILITARY ACTIVITY
TECH, OTHER	AF Office of Scientific Research (NAE) 1400 Wilson Boulevard Arlington, Virginia 22209

13. ABSTRACT

Theoretical and experimental studies were performed to obtain fundamental understanding of initiation and propagation of low-velocity detonation (LVD) in confined energetic liquids. LVD was modeled as a reactive shock propagation in a liquid cavitated by interactions with the container wall. Reaction required to support the wave in this cavitation model is initiated by bubble collapse in the compressed cavitation field. 2-D computer studies of a shock propagating in a contained liquid showed precursor wall waves produce regions of tension sufficient to cavitate the liquid before it is compressed by the main shock. Simulation of hot-spot-initiated reaction by addition of energy behind the shock substantiated the hypothesis of partial energy release in LVD. Methods of calculating LVD parameters were formulated with the hydrothermodynamics of the cavitation model, and a complete equation of state for nitromethane was introduced into the TIGER code to permit detonation calculations for incomplete reaction. Calculations showed about 20 percent of liquid is required to support LVD. Dynamics of collapsing vapor bubbles were analyzed to study hot-spot reaction intiation and conditions for LVD initiation. Initial rate of temperature increase in bubbles with heat and mass transfer was found to be 10 to 20 times less than in bubbles without transfer at the bubble wall. Pressure-time histories obtained in confined shocked monopropellants showed shock decay, initiation of LVD, and the initiation of high-velocity detonation. LVD peak pressures were 4- to 7-kbar, and LVD velocities were about 2.0 mm/μsec in ethyl nitrate and 3.0 mm/μsec in FEFO.

DD FORM 1 NOV 68 1473

UNCLASSIFIED

Security Classification

UNCLASSIFIED

Security Classification

14 KEY WORDS	LINK A		LINK B		LINK C	
	ROLE	WT	ROLE	WT	ROLE	WT
MONOPROPELLANTS						
LOW VELOCITY DETONATION						
CAVITATION						
REACTIVE WAVE PROPAGATION						
HYDROTHERMODYNAMICS						
EQUATION OF STATE						
HUGONIOT CURVES						
DEFLAGRATION						
INCOMPLETE REACTION						
BUBBLE DYNAMICS						
HEAT AND MASS TRANSFER						
SHOCK INITIATION						
YTTERBIUM STRESS GAGES						
PRESSURE MEASUREMENTS						

UNCLASSIFIED

Security Classification

ABSTRACT

Theoretical and experimental studies were performed to obtain a fundamental understanding of the initiation and propagation of low-velocity detonation (LVD) in confined energetic liquids. LVD was modeled as a reactive shock propagating in a liquid cavitated by interactions with the container wall. The reaction required to support the wave in this cavitation model is initiated by bubble collapse in the compressed cavitation field.

Two-dimensional computer studies of a shock propagating in a liquid contained in a cylindrical steel tube showed that precursor wall waves produce regions of tension sufficient to cavitate the liquid before it is compressed by the main shock. Simulation of hot-spot-initiated reaction by addition of energy behind the shock substantiated the hypothesis of partial energy release in LVD. Methods of calculating LVD parameters were formulated with the hydrothermodynamics of the cavitation model, and a complete equation of state for nitromethane was introduced into the TIGER code so that detonation calculations could be made for incomplete reaction. The calculations showed that only about 20 percent of the liquid is required to react to support LVD. The dynamics of a collapsing vapor bubble were analyzed to study the hot-spot initiation of reaction and the conditions for initiation of LVD. The initial rate of temperature increase in a bubble with heat and mass transfer was shown in general to be 10 to 20 times less than that in a bubble without transfer at the wall.

Experimental studies resulted in measurements of pressure in LVD. Pressure-time histories in shocked monopropellants contained in cylindrical steel tubes were recorded by piezoresistant ytterbium in-material stress gages. Gage records obtained by varying the monopropellant, the wall

thickness-to-diameter ratio of the tube, and the initial shock pressure showed shock decay, initiation of LVD, and the initiation of high-velocity detonation. The peak pressures recorded by LVD were in the 4- to 7-kbar range, and the LVD velocities of propagation were about 2.0 mm/μsec in ethyl nitrate and 3.0 mm/μsec in FEFO.

CONTENTS

I INTRODUCTION

This report presents the results of a three-year theoretical and experimental program whose objective was to obtain a fundamental understanding of low-velocity detonation (LVD) phenomena in liquid propellants, fuels, and explosives. Low-velocity detonation occurs in confined, highly energetic liquids. It can be initiated by much smaller shock impulses than can high-velocity detonation (HVD), but can cause considerable damage. Present hydrothermodynamic detonation theory predicts the existence of only HVD for any particular thermodynamic state of the explosive. The existence of LVD therefore represents an anomaly heretofore unexplained in detonation theory. A basic understanding of LVD is of great practical significance in establishing safety requirements for the handling of liquid fuels, propellants, and explosives.

The following tasks were accomplished during the research program:

(1) A complete literature review and a reevaluation of existing LVD data were accomplished to identify the individual mechanisms contributing to LVD initiation and propagation. The experimentally observed features of LVD were identified and used to evaluate the various models of LVD that have been proposed. A model that offered the most plausible explanation of the phenomenon and that was consistent with the experimental observation was adopted as a starting point for the subsequent work. This model was called the cavitation model of LVD.

(2) A preliminary theoretical analysis of the interaction of the confinement system with the liquid explosive was carried out. The studies established that precursor wall waves capable of causing cavitation in the liquid ahead of the main liquid shock are possible.

(3) The physical and chemical properties of liquids known to undergo LVD, as well as those in which LVD was not observed, were examined. The results of this task suggested the significance of cavitation in the LVD phenomenon.

(4) Detailed computer calculations utilizing the cavitation model of LVD were carried out to study the cavitation production mechanism, the effects of partial energy release, the initiation of LVD, and the possible transition of LVD to HVD.

(5) A hydrothermodynamic treatment of the cavitation model of LVD was undertaken in an attempt to develop a satisfactory method for calculating LVD propagation velocity. Interaction of the shock and the cavitation field was accounted for simply by ordering the time scales for the attainment of mechanical, thermal, and chemical equilibrium. Since results based on the attainment of chemical equilibrium did not agree with experiment, the case of incomplete reaction was considered.

(6) Characteristic times for bubble collapse, heat transfer within a bubble, and heat transfer to the surrounding liquid were compared to assess the relative rates of possible processes occurring in the compressed cavitation field. The initial collapse of a vapor bubble was treated analytically in an attempt to obtain a more detailed account of bubble dynamics and to determine conditions for the onset of reaction and the initiation of LVD.

(7) Experiments using metriol trinitrate (TMETN) were carried out to examine the effects of confinement upon LVD initiation and propagation.

(8) Experiments were carried out to measure the stress field ahead of and during the passage of the liquid shock. Detonation velocity measurements as well as damage criteria were used to verify the observed LVD phenomenon.

As a result of the above studies, a quantitative model of LVD has been developed that is consistent with the experimentally observed properties of LVD. Further, experimental verification of some of the more important quantitative predictions of the model has been carried out.

The results of this work, intended for publication in technical journals, are presented in the manuscripts attached as Appendices to this report, and a complete list of references of the work performed during the present research program is given in the Bibliography.

II ASSESSMENT OF PAST WORK

For most practical applications, condensed explosives are required to behave reproducibly, to undergo HVD, and to produce pressures in the 100-kbar region. As a result, investigations of detonation phenomena have been focused largely on HVD--rather than on LVD, which produces pressures in the 10-kbar region. Consequently, at the beginning of this research program, the conditions for initiation and propagation of LVD were not as well established as were those for initiation and propagation of HVD. This disparity in our understanding was accentuated by the fact that previous experimental studies of LVD had produced only limited results, generally of a qualitative nature. For instance, it was clear that a reactive wave traveling at about sonic speed in virgin explosive was associated with stable LVD, that LVD could be initiated more easily than HVD, and that initiation depended on the properties and geometry of the container holding the explosive. There was, however, no physical model for LVD corresponding to the Zeldovich-vonNeumann-Doering model[1-3*] for HVD. Neither were there criteria for calculating detonation velocity from the properties of the explosives corresponding to the Chapman-Jouguet (C-J) hypothesis nor a satisfactory model for treating the coupling between the container walls and the explosive in the LVD process.

During the initial stages of this program, a comprehensive survey and evaluation was made of existing experimental data and theoretical models pertaining to LVD. The results of this study are given in detail

*References are listed at the end of the report.

in the first annual report.[4] Although rather extensive literature on LVD was known to exist, it was recognized at the outset that most past observations had been scattered and uncoordinated. Among the U.S., European, and Soviet investigators who had previously studied LVD phenomena, there was little agreement concerning the validity of much of the reported work. Moreover, there had been no very thorough attempts to resolve the conflicts. Accordingly, the program began with an effort to delineate the really important factors contributing to LVD and to discard those concepts and measurements that have tended to confuse the issue. The objective of this initial study was to establish the direction to be taken in planning and executing the rest of the investigation.

Each of the surprisingly numerous existing conceptual models of LVD initiation and propagation was first examined against the background of accumulated data. Many concepts were thus shown to be highly improbable and unworthy of further study. The remaining concepts, which seemed reasonably consistent with experimental information, were subjected to fairly simple analyses as a further test of their validity and relevance for subsequent research in this program.

Apart from quantitative disagreements with available data, most models failed to explain certain important and experimentally well-established physical characteristics of LVD, such as the marked influence of container geometry and material (strength) on the initiation and stability of LVD waves. Two conceptual models that had been proposed seemed qualitatively consistent with these behavior characteristics and therefore deserved careful consideration.

Amster et al.[5] suggested the possibility of hot-spot initiation induced by a Mach disk (local normal shock) occurring at the center of the container when precursor shocks generated by container wall deflections

converge along the centerline. Although this model affords a plausible explanation of certain behavioral characteristics, a recent analysis at Stanford Research Institute (SRI) indicates that the Mach disk generally is not strong enough to create the local temperatures needed for initiation. The hot-spot initiation concept was retained in a model first suggested by Watson et al.[6] Their model, which qualitatively fits existing experimental observations, envisioned the appearance of cavitation in the liquid, followed by a shock wave that collapses the bubbles, causing local hot spots that act as initiation centers. Watson[7] had also taken photographs showing cavitation ahead of the reaction zone, and Watson et al.[8] had more recently reported measurements of elastic precursor wall waves that further substantiate the cavitation model of LVD. Based upon the work done at SRI under this program[4,9] and in light of the properties of LVD observed to date by others, the cavitation model appeared to offer the most plausible mechanism for the propagation of LVD.

The cavitation model for LVD assumes that container interaction with the energetic liquid produces cavitation ahead of a shock in the liquid. The liquid shock subsequently compresses the bubbles, causing initiation and subsequent burning. The approach taken in this program to develop a better theoretical understanding of the LVD phenomenon has been to examine the mechanisms by which cavitation is produced in the liquid and theoretically to model the reaction zone in an attempt to predict observed LVD behavior. This theoretical work was supplemented by experiments designed to test the analytical model critically. In the following, the work on the cavitation production mechanism, the theoretical modeling of LVD, and the experimental results are summarized.

III LVD COMPUTER MODEL - WALL INTERACTION PRODUCING CAVITATION

The validity of the cavitation model of LVD requires that a mechanism exists for the production of cavitation in the liquid ahead of the LVD wave. As a part of the current program, an analysis of the liquid-wall interaction was performed to determine whether significant cavitation should indeed occur. In a simplified preliminary analysis, it was found that precursor shocks in the container walls can cause a container wall-liquid interaction capable of producing a substantial degree of cavitation in the liquid.[4] This analysis was carried further by a computer calculation using SRI's two-dimensional shock code to calculate the stresses produced in a liquid contained in a cylindrical steel pipe or tube when shocked at one end. Large tensile stresses were produced in the liquid across its entire cross section by the wall interaction. The results show that large degrees of cavitation can be produced in the liquid. This cavitation and the resulting possibility of hot-spot initiations are very important, not only for LVD, but for the initiation of HVD in liquid (and even some solid) explosives.

The calculations of stress wave propagation down a liquid-filled cylindrical tube, impacted at one end, were made using SRI's FIBROUS computer code. FIBROUS is a two-dimensional finite-difference code modeled after the description of Wilkins,[10] that can handle both elastic-plastic and purely hydrodynamic constitutive relations.

To study further the cavitation model of LVD, the stress history was computed for a liquid explosive contained in a cylindrical steel container subsequent to its being impacted at one end. The results of the computations show that coupling between the container wall and the liquid produces precursor tension zones in the liquid leading to cavitation

ahead of the main liquid shock and that recompression of the cavitated zones by the liquid shock is sufficient to initiate reaction to support the propagation of the liquid shock. The simulation for ethyl nitrate in a 1-inch I.D. by 1/8-inch wall thickness steel pipe resulted in detonation velocities of about 1.8, 2.4, and 3.0 mm/μsec, respectively, for energy releases of 0, 0.4, and 1.0 times the heat of reaction. Since experimental LVD propagates at about 2 mm/μsec, this was taken as evidence of partial energy release in LVD. The results of this work showed the details of the cavitation production and recompression and further substantiated the cavitation model of LVD.

The computer model of LVD provides a means for studies of initiation and propagation of LVD in various confinement systems and, in addition, has provided valuable information about the initiation and propagation of LVD. The results of the computer modeling of LVD are fully described in Appendix A.

IV HYDROTHERMODYNAMICS OF THE CAVITATION MODEL OF LVD

Our cavitation model for LVD is a reactive shock propagating in a cavitated liquid. Propagation is thus a very complex phenomenon involving the formation of a cavitation field and its subsequent behavior under shock compression. The most important problem in a theoretical treatment of LVD is that of calculating the velocity of propagation. Such calculations must take account of liquid-container wall interaction, and the dynamics and thermodynamics of cavitation bubbles with heat transfer, mass transfer, and chemical reaction. The simplest treatment of these processes was used in the initial work to develop a method of calculating LVD velocity. Our approach was motivated by the fact that the classical C-J hypothesis is satisfactory for calculating the detonation velocity in gases even though a gaseous detonation wave consists of a complex system of interacting shock waves. In the simplest treatment of LVD, the cavitation field in virgin liquid is formed quickly through liquid-container interactions, and is accounted for only by the initial conditions for shock propagation; the compressed cavitation field is assumed to be in mechanical equilibrium and to form a steady-state reaction zone terminating in a state of complete reaction.

It was demonstrated that the LVD velocity is uniquely determined by our assumptions. With our assumption of cavitation, the shock is represented by a Rayleigh line passing through the initial condition of the cavitated liquid and not the initial condition of the liquid. With the assumption of mechanical equilibrium in the compressed mixture of bubbles and liquid, there is a well-defined pressure at each point of the reaction zone, and the initial state for the burning is the initial shocked condition in the cavitated liquid. With the assumption of complete reaction, the end of the reaction zone lies on the equilibrium products Hugoniot curve centered on the initial shocked condition of the cavitation liquid.

For the initial, simplest treatment of the cavitation model, LVD propagation velocity is determined by the C-J condition on the equilibrium products Hugoniot curve centered on the cavitated liquid.

The TIGER code was used to calculate detonation parameters in ethyl nitrate for different degrees of cavitation, and the results of these calculations are shown in Table 1. The internal energy of the cavitated liquid ahead of the shock was assumed to be the same as that of the uncavitated liquid. Calculations with the BKW and virial equations of state do not agree with experiment; propagation velocities calculated with the ideal gas equation of state agree with experiment, but detonation pressures lie in the kilobar region where this equation of state is inapplicable.

The results of the calculations led to the conclusion that the initial assumptions were too restrictive. A more sophisticated treatment of the compressed cavitation field was required to model LVD. Thus, a more detailed study of bubble collapse, heat and mass transfer, and chemical reaction was undertaken to achieve this objective. In addition, a modification of the TIGER code to allow partial energy release was used to examine a less restrictive model and to determine the amount of reaction required to support LVD. The hydrothermodynamic treatment of the cavitation model of LVD is discussed in greater detail in the manuscript of a technical paper attached as Appendix B.

Table 1

Detonation Parameters in Ethyl Nitrate Calculated with the TIGER Code

Equation of State	Initial Volume (cc/gm)	Detonation Velocity (mm/μsec)	C-J Particle Velocity (mm/μsec)	C-J Pressure (kbar)	C-J Volume (cc/gm)	C-J Temperature (°K)
BKW	0.905 *	6.73	1.81	132.8	0.66	2608
	1.77	4.80	1.48	39.6	1.23	2666
	2.03	4.56	1.43	31.7	1.39	2625
	2.37	4.31	1.37	24.6	1.61	2585
	2.82	4.04	1.31	18.53	1.91	2572
VIRIAL**	0.905*	4.02	1.31	57.0	0.61	3277
	1.77	3.36	1.16	21.7	1.16	2981
	2.03	3.25	1.14	18.0	1.32	2930
	2.37	3.14	1.11	14.6	1.53	2878
	2.82	3.02	1.09	11.5	1.81	2827
IDEAL GAS	0.905*	2.22	1.00	17.0	--	--
	1.77	2.22	1.00	12.2	0.98	2728
	2.03	2.22	1.00	10.6	1.12	2718
	2.37	2.22	1.00	9.1	1.31	2708
	2.82	2.22	1.00	7.6	1.56	2698

* Detonation in virgin material (no cavitation).
** Third virial coefficient set equal to zero.

V BUBBLE DYNAMICS

In the initial study of bubble dynamics, the characteristic times for bubble collapse,[11] heat transfer within a bubble, and heat transfer to the liquid were compared as a means of assessing the relative rates of relaxation processes occurring in the compressed cavitation field behind the shock. The collapse of a bubble was then treated in more detail in an attempt to determine conditions for the onset of reaction and the initiation of LVD.

The dynamics of the collapse of a vapor bubble were analyzed to study the hot-spot initiation mechanism essential to the cavitation model of LVD. The temperature distributions in a collapsing spherical vapor bubble and in the surrounding liquid were computed. Gas-phase reaction, heat and mass transfer at the bubble wall, and motion of the bubble wall were included in the computations in order to simulate closely the thermal history of a collapsing vapor bubble and the criteria for hot-spot initiation. A vapor bubble was studied since during the very rapid cavitation that occurs in liquids undergoing LVD, even if dissolved gases such as air are present, there is not sufficient time for diffusion into the resulting cavity. Thus, cavitated zones under such conditions would consist of vapor bubbles containing negligible amounts of gas.

This work on bubble collapse leading to hot-spot initiation is discussed in detail in Appendix D.

VI EXPERIMENTAL RESULTS

As a part of the studies of LVD undertaken in this program, three separate sets of experiments were carried out to substantiate the theoretical model and to further delineate the important mechanisms that occur in the initiation and propagation of LVD. The objective of the first experiment was to study the role of confinement, that of the second set of experiments was to measure the wall stress just ahead of the detonation wave, and in the third set of experiments detailed measurements were made of the stress in the liquid ahead of and during the passage of the leading LVD-associated shock wave. The detailed description of these experiments and the results obtained are described in the first and second annual reports and Appendix E.

In summary, the first set of experiments were run using metriol trinitrate (TMETN) in steel tubes of various diameter and wall thicknesses. For each configuration LVD velocity was measured down the tube for various input shock strengths. Once the proper initiating shock was determined for a nominal 1/8-inch wall tube, the wall thickness was varied keeping all other conditions constant. Weaker confinement generally resulted in decay of the LVD wave as it propagated down the tube, and stronger confinement resulted in transition to HVD. The important role of circumferential or hoop stress in the cavitation mechanism, as predicted by theory, was confirmed by experiments using a tube with an axial slit down one side.

In the second set of experiments, a limited number of shots were made, again using TMETN, to measure wall stress ahead of the main LVD shock. Deformation and ringing of the wall were observed, also in agreement with theory.

The most recent experiments, designed to measure the pressure in the liquid ahead of and during passage of the LVD wave, were run using several liquids and with 1-inch and 3/4-inch I.D. steel tubes. The measured pressures were in close agreement with the pressures calculated by the computer model. Appendix E provides a detailed discussion of this work.

In general, the close agreement between experimental results and theoretical predictions based upon the cavitation model of LVD further supports the cavitation model and provides a better understanding of the LVD phenomenon. In addition, this capability gives a good basis for further research.

VII BIBLIOGRAPHY

1. D. C. Wooten, H. R. Bredfeldt, R. W. Woolfolk, and R. J. Kier, "Investigation of Low-Velocity Detonation Phenomena in Liquid Propellants, Fuels, and Explosives," Annual Report, AFOSR Scientific Report AFOSR 70-1005TR, March 1970.

2. D. C. Wooten and M. Cowperthwaite, "Investigation of Low-Velocity Detonation Phenomena in Liquid Propellants, Fuels and Explosives," Annual Progress Report, AFOSR Contract No. F44620-69-C-0079, April 1971.

3. D. C. Wooten, M. Cowperthwaite, and D. C. Erlich, "Investigation of Low-Velocity Detonation Phenomena in Liquid Propellants, Fuels, and Explosives," Final Report, AFOSR Contract No. F44620-69-C-0079.

4. D. C. Wooten and D. C. Erlich, "The Wave Structure in Shocked, Confined Explosives Associated with Low-Velocity Detonation," (to be published).

5. D. C. Wooten, "Collapse of a Vapor Bubble Leading to Hot-Spot Initiation" (to be submitted for publication).

6. D. C. Erlich and D. C. Wooten, "Measurement of Pressure in a Liquid Explosive Undergoing Low-Velocity Detonation" (to be submitted for publication.

7. M. Cowperthwaite, "Hydrothermodynamics of the Cavitation Model of Low-Velocity Detonation" (submitted for publication).

8. R. W. Woolfolk, M. Cowperthwaite, and R. Shaw, "A 'Universal' Hugoniot for Liquids" (submitted for publication).

REFERENCES

1. Ya. B. Zeldovich, Sov. Phys.-JETP 10, 542 (1940).

2. J. von Neumann, Theory of Detonation Waves, OSRD No. 549 (1942).

3. W. Doering, Ann. Phys. 43, 421 (1943).

4. D. C. Wooten, H. R. Bredfeldt, R. W. Woolfolk, and R. J. Kier, "Investigation of Low-Velocity Detonation Phenomena in Liquid Propellants, Fuels, and Explosives," Annual Report, AFOSR Scientific Report AFOSR 70-1005TR, March 1970.

5. A. B. Amster, D. M. McEachern, Jr., and Z. Pressman, "Detonation of Nitromethanes-Tetranitromethane Mixtures: Low and High Velocity Waves," Proceedings, Fourth Symposium (International) on Detonation, ACR-126; Office of Naval Research, Department of the Navy, Washington, D.C., p. 126.

6. R. W. Watson, C. R. Summers, F. C. Gibson, and R. W. Van Dolah, "Detonations in Liquid Explosive--The Low-Velocity Regime," Proceedings, Fourth Symposium (International) on Detonation, ACR-126; Office of Naval Research, Department of the Navy, Washington, D.C., p. 117.

7. R. W. Watson, "The Structure of Low Velocity Detonation Waves," Twelfth Symposium (International) on Combustion, The Combustion Institute, Pittsburgh, 1969, p. 723.

8. R. W. Watson, J. Ribovich, J. E. Hay, and R. W. Van Dolah, "The Stability of Low-Velocity Detonation Waves," Fifth Symposium (International) on Detonation, August 18-21, 1970, p. 71 (ONR Report DR-163).

9. D. C. Wooten and M. Cowperthwaite, "Investigation of Low-Velocity Detonation Phenomena in Liquid Propellants, Fuels, and Explosives," Annual Progress Report, AFOSR Contract F44620-69-C-0079, April 1971.

10. M. L. Wilkins, Calculation of Elastic-Plastic Flow, Methods of Computational Physics, Vol. III (Fundamental Methods in Hydrodynamics), p. 211, Eds. B. Alder, S. Fernbach, M. Rottenberg, Academic Press, New York (1964).

11. R. Hickling and M. S. Plesset, "Collapse and Rebound of a Spherical Bubble in Water," Phys. Fluids 7, 7 (1964).

Appendix A

THE WAVE STRUCTURE IN SHOCKED, CONFINED LIQUIDS ASSOCIATED WITH LOW-VELOCITY DETONATION

THE WAVE STRUCTURE IN SHOCKED, CONFINED LIQUIDS ASSOCIATED WITH LOW-VELOCITY DETONATION*

by

David C. Wooten
Ultrasystems, Inc.
Newport Beach, California

and

David C. Erlich
Stanford Research Institute
Menlo Park, California

February 1972

*This work was supported by the U.S. Air Force Office of Scientific Research under Contract No. F4462-69-C-0079

ABSTRACT

To study the cavitation model of low-velocity detonation (LVD), the stress history is computed for a liquid explosive contained in a cylindrical steel container, subsequent to its being impacted at one end. It is shown that coupling between the container wall and the liquid produces precursor tension zones in the liquid leading to cavitation ahead of the main liquid shock. Recompression of the cavitated zones by the liquid shock, in accordance with the cavitation LVD model, is assumed to cause hot-spot initiation of the liquid, and the subsequent energy release in turn supports the liquid shock. The simulation for ethyl nitrate in a 1-inch I.D. by 1/8-inch wall thickness steel pipe resulted in detonation velocities of about 1.8, 2.4, and 3.0 mm/μsec, respectively, for energy releases of 0.1, 0.4, and 1.0 times the heat of reaction. Since experimental LVD propagates at about 2 mm/μsec, this is taken as evidence of partial energy release in LVD. The results show the details of cavitation and recompression and further substantiate the cavitation model of LVD.

Introduction and Background

Low-velocity detonation (LVD) is a low-order detonation phenomenon that is observed in liquid explosives under particular conditions of confinement. In 1919 LVD was first observed in nitroglycerine by Stettbacker.[1] Until the past decade, however, the phenomenon remained relatively obscure and there was little agreement among investigators concerning the observed properties of LVD. More recently, because of the increasing uses of highly energetic liquids as propellants, fuels, and explosives--many of which are known to be susceptible to LVD--a number of investigations of LVD have been undertaken. As a result of these studies, the important characteristics of LVD are becoming well defined, and plausible explanations of the observed phenomena have emerged.

Experiments indicate that LVD can occur in almost any highly energetic monopropellant. Typically, LVD propagates at speeds only slightly greater than the liquid sound speed or in the range of 1.5 to 2.5 mm/μsec. Stable LVD is in general observed only in strongly confined explosive systems and only if the sound speed of the container wall material exceeds that of the undisturbed liquid. On the other hand, in the very weak containers and in containers with wall sound speeds less than that of the liquid, an unstable LVD is sometimes observed which propagates in a pulsating manner with an average speed that is subsonic relative to the liquid. Unstable LVD typically propagates only a short distance before dying out.

Though both types of detonation are observed in some liquids, the observed properties of LVD are distinctly different from those of HVD.

In addition, energetic liquids are generally much more sensitive to LVD initiation; LVD may be initiated by shock overpressures on the order of 1 to 5 kbar while shocks of 50 to 100 kbar are usually required to initiate HVD. Moreover, above a certain minimum charge diameter, HVD propagation characteristics are independent of confinement whereas LVD is strongly dependent upon both confinement geometry and the properties of the wall material. Thus, LVD represents a stable, low-order detonation wave, the HVD wave. Over the years, a number of models of the LVD phenomenon have been proposed but, until recently, attempts to explain LVD theoretically have met with little success. Stettbacker,[1] in an attempt to explain his early observations, and later Deserhkovich and Andreev[2] suggested that the two detonation velocities in nigroglycerine were related to two known crystalline forms of the solid. More recently, in a theoretical paper, Bolkhovitinov[3] attempted to explain LVD on the basis that a phase transition from liquid to solid takes place behind the initiating shock. In addition, as a part of their study of hot-spot initiation in explosives, Bowden and Gurton[4] suggested that energy losses due to lateral expansion in the reaction zone give rise to LVD behavior. These theories, although predicting a low-order detonation, do not account for the experimentally observed characteristics of LVD, particularly that the sound speed in the container material must be greater than that in the liquid.

In contrast to the above phenomenological theories, a model of LVD based on purely thermodynamic theory by Eyring et al.[5] and a similar approach taken later by Evans[6] utilized a variable-reaction-zone length which depended upon detonation velocity. These models predict the existence of two detonation velocities but the resulting LVD velocity varies inversely with charge diameter, a fact which is not supported by experimental evidence. An attempt to explain the LVD phenomenon with a

semiempirical model based on varying energy release rates behind the initiating shock was given by Schall[7] who suggested that disturbed gas bubbles distributed in the liquid might account for the energy release rates responsible for LVD. While each thermodynamic model of LVD predicts a low-order detonation velocity, they all fail to explain the experimentally observed characteristics of LVD, especially that LVD is observed in many liquid compounds with different physical properties, propagates with approximately the same detonation velocity independently of the compound, and is apparently strongly coupled to the confinement system.

Recognition of the close interrelationship between LVD properties, such as the ease of initiation, stability, and detonation speed, and the charge confinement characteristics, such as container geometry, strength, and elastic properties of the wall material, has led to models of LVD which include detonation wave-wall coupling. One model, for example, that accounted for the empirical interrelationship between LVD incidence and container wall characteristics was given by Woolfolk and Amster[8] who suggested that the container wall shock causes pressure waves in the liquid which converge at the center to produce a Mach disk capable of initiating detonation. However, in this model, the wall shock and therefore the Mach disk would continuously outdistance the LVD wave unless the LVD were moving at a speed higher than that observed.

Another empirical model which also utilizes coupling between the wall and the detonation and which seems to fit the experimentally observed facts was recently suggested by Watson et al.[9] and independently by Voskoboinikov et al.[10] In this model, precursor waves in the container wall cavitate the liquid ahead of a liquid shock. The cavitation bubbles are subsequently compressed by the liquid shock causing a hot-spot-initiated reaction, and the resulting energy release in turn drives the

shock. This model has been further verified by Watson[11] who has taken photographs of cavitation ahead of the reaction zone and by Watson et al.[12] who more recently have reported tentative measurements of precursor wall waves capable of producing cavitation ahead of the reaction zone. In addition, the existence of individual burning sites rather than a continuous reaction front has been observed by Watson[11] in X-ray photographs of the LVD reaction wave, and Gibson et al.[13,14] have experimentally verified the dependence of bubble ignition on the strength of the initiating shock. The cavitation model also explains the relatively long dark region observed between the shock front and the luminescent reaction zone.[11] Thus, the cavitation model, though it involves an incompletely understood interaction between the container and the liquid explosive to produce cavitation and subsequent hot-spot reaction and as yet unknown criteria for stability, appears to offer the most plausible mechanism for the propagation of LVD.

Our purpose here is, on the basis of the cavitation model, to examine cavitation and recompression mechanisms in both the initiation and propagation of LVD. A computer simulation of the cavitation model of LVD is utilized to study the stress history in a system consisting of a liquid explosive in a cylindrical container subsequent to being shocked at one end. The hot-spot-initiated reaction is simulated by energy release when a precavitated zone in the liquid is recompressed above a threshold level by the main liquid shock. The results help clarify the liquid-wall interaction mechanism that leads to precursor cavitation and the subsequent collapse of the cavities by the liquid shock, and further substantiates the cavitation model of LVD.

Cavitation Model of LVD

Experimental sutdies of LVD are usually carried out in an arrangement similar to that used to study the sensitivity of liquid explosives.[15] The liquid to be studied 's placed in a container, most often a cylindrical tube, which is shocked at one end by an explosive donor. The strength of the initiating shock can be varied by using attenuators (usually Lucite) of different thicknesses. For a number of liquids, initiating shocks on the order of 1 to 10 kbar typically produce LVD whereas much stronger shocks, on the order of 100 kbar, directly initiate HVD. Experimenters in the past have studied LVD phenomena with high-speed cameras, velocity-measuring probes, and strain gages to measure circumferential wall strain.[8-12]

When the initiating donor shock wave impacts the explosive system, the shocks produced propagate down the cylinder from the donor end. If the sound speed in the container wall material is greater than that in the liquid, then the wall shock outdistances the liquid shock and causes a precursor wave system ahead of the liquid shock. Calculations discussed in the following sections show that these precursor waves cause zones of tension capable of cavitating the liquid. The cavitated liquid is subsequently recompressed by the liquid shock leading to the possibility of hot-spot initiation. This mechanism is probably the manner in which LVD initiation takes place and under some conditions as, for example, for a stronger donor shock, could lead to HVD initiation. The calculations demonstrate that relatively weak donor shocks, on the order of 1 kbar, are sufficient to produce significant cavitation in the liquid, thus accounting for the high shock sensitivity of liquid explosives to hot-spot initiation and to LVD.

The cavitation model of LVD requires that precursor wall waves produce tension zones leading to cavitation ahead of the liquid shock. If the wall shock caused by the donor were the only mechanism for cavitating the liquid, then all LVD waves would be inherently unsteady, since in the experimental conditions where stable LVD is observed, the wall shock continually outdistances the LVD waves. However, if the wall deflection due to the LVD wave itself is capable of producing precursor cavitation, then a self-sustaining, steady LVD is possible. Though Watson et al.[11] report some preliminary experimental evidence that there is a precursor pressure wave attached to the reaction zone, it has not been established that such a mechanism leads to precursor cavitation. In either case, it is clear that when the sound speed in the container wall material is less than that in the liquid, precursor wall waves caused by either the donor shock or the LVD wave are not possible.

Pulsating LVD is sometimes observed when the wall sound speed is only slightly greater than that of the liquid;[12] it may occur when the complex interaction between the donor and the receptor causes hot-spot initiation which starts to accelerate toward a full LVD. Subsequently, as the resulting reaction wave approaches the wall sound speed there is no mechanism for the generation of precursor cavitation and the reaction dies out from the lack of initiation centers. As the reaction zone slows down due to decreased energy release rate, the wall wave may again outdistance it, once again causing cavitation ahead of the reaction zone. The whole process may then repeat itself in an oscillatory fashion resulting in pulsatory LVD. Clearly, whether such an unstable LVD will continue to propagate must depend critically upon the experimental conditions. In fact, unsteady LVD is frequently observed to die out altogether.

Computer Simulation

A computer study of cavitation and recompression in an energetic liquid contained in a cylindrically symmetric tube impacted at one end was undertaken in an attempt to simulate the initiation and propagation of LVD. Ethyl nitrate, contained in a 1-inch I.D. by 1/8-inch wall cylindrical steel tube, was chosen for the calculations as being representative of a typical experimental setup used to study the shock initiation of LVD in the practical part of the research program. Of particular interest in these calculations are the following factors:

(1) Does the stress wave traveling down the pipe walls create a region of tension in the liquid sufficient to produce cavitation ahead of the main compression wave in the liquid?

(2) What is the propagation velocity of LVD and how does it depend upon the amount of energy released in the reaction zone?

(3) Is a stable LVD wave (one that propagates at a constant velocity) established at some distance (equal to several pipe diameters) down the pipe?

Computer simulations were performed using the SRI FIBROUS code. This code is a two-dimensional finite difference stress wave propagation code modeled after the description of Wilkins,[16] that includes both elastic-plastic and hydrodynamic constitutive relations. When the FIBROUS code is used in the axially symmetrical geometry, a rectangular grid parallel to the axis of the cylinder extending from the axis to the edge of the cylinder is specified, as shown in Figure 1. The code treats each cell of this plane grid as if it contained the volume swept out by the 360-degree rotation of the grid about the cylindrical axis.

A similar projectile cylinder impacts the target from the right to begin the computation. (The shock produced in the explosive system by the projectile cylinder simulates the shock delivered in the experimental setup by the donor-attenuator.) At successive time increments after impact, all of the relevant parameters needed to characterize the stress wave propagation are calculated for each grid cell. These include position, velocity, triaxial stresses, hydrodynamic pressure, internal energy, and specific volume. Certain specified parameters at designated cells can be stored by the computer at each time increment, and these can be tabulated or plotted at the end of the calculation to give, for example, stress and specific volume histories, or stress-volume loading and unloading paths.

For each cell during each cycle the calculation proceeds basically as follows: the stresses in the adjacent cells during the previous cycle are used to compute the current acceleration for the cell which, along with its previous velocity and position, is then used to compute its current velocity and position. From the latter are obtained the current triaxial strains, distortional strain energy, and the specific volume which--together with the equation of state or constitutive relation of the material in the cell--are used to compute the current triaxial stresses, the hydrostatic pressure, and the internal energy. The Mie-Grüneisen[17] equation of state is used to relate changes in the internal energy to changes in the hydrostatic pressure. The time increment between successive cycles is chosen so that a stress wave propagates less than the distance between two cells during that time.

The computational grid for the simulation of LVD was set up as in Figure 1.* The target grid contained 4 rows of liquid cells and one row of steel pipe cells in the radial direction; each row contained 97 cells

* The figures are shown at the end of this appendix.

in the axial direction. However, only about the first half of the target in the axial direction yielded useful stress histories in the liquid cells, since reflection of the stress wave in the pipe wall from the free surface disrupted the stress flow in the latter half of the target. Therefore the usable LVD simulation calculations were carried out only to about 6 diameters down the tube. The projectile, which contained 5 rows of cells in the radial direction with each row containing 10 cells in the axial direction, impacted the target at a velocity of 0.5 mm/μsec. The cells for both the target and projectile grids were 3 mm square.

An elastic-plastic equation-of-state formulation for Armco iron[18] was used for the constitutive relations for the steel pipe cells. It included a nonlinear hydrostatic pressure-specific volume (P-V) Hugoniot curve given by

$$P = 1{,}590\,\mu + 5{,}170\,\mu^2 + 51{,}700\,\mu^3 ,$$

where $\mu = \frac{V_o}{V} - 1$, P is in kbar and $V = 0.1274$ cm^3/gm. A shear strength of 7.9 kbar and a shear modulus of 820 kbar were used. The equation of state for water was used for the liquid cells, inasmuch as the density and shock properties of water are similar to those of the liquid propellants of interest in LVD studies. The hydrostatic pressure of the liquid was defined by

$$P = 25.6\mu + 61.2\mu^2 + 122.7\mu^3 .$$

It was found that when a purely hydrodynamic equation of state (one in which the shear strength is zero) is used for the liquid, the liquid cells next to the wall become highly elongated because liquid in the center of the tube tends to flow down the tube whereas the liquid adjacent to the wall is prevented from sliding along the inside of the wall (no sliding interfaces are allowed in the FIBROUS code). Since a

highly elongated cell, particularly one in which one diagonal is much larger than the other, may lead to calculational inaccuracies, the liquid was given a small shear strength of 0.1 kbar. It is not expected that this had any significant effect upon the simulation. The equation of state of C-7 was used for the constitutive relations for the projectile material. It will not be described here, since the projectile equation of state has no effect upon the stress history for time intervals relevant to the LVD simulation.

The cavitation of the liquid ahead of the liquid stress wave and the subsequent detonation of the cavitated liquid upon arrival of the liquid shock were simulated in the following manner: whenever the tensile stress (pressure) in a cell of the liquid exceeded 0.02 kbar, this cell was tagged and the tensile stress was reset to 0.02 kbar. So when further tensile strain was applied to this cell, the cell continued to expand at a constant negative pressure level of 0.02 kbar. This approximation to the liquid stress-strain behavior during cavitation was handled with only minor adjustment to the FIBROUS code. A more realistic treatment of cavitation that is possible but involves more substantial changes in the FIBROUS code will be discussed below.

All of these tagged cells (which had undergone negative stress in excess of 0.02 kbar and hence cavitation) subsequently experienced recompression due to the arrival of the main compressional wave in the liquid. When the pressure in the tagged cells exceeded 0.4 kbar in compression, an amount of energy equal to the energy that is expected to be released by the hot-spot reaction was added to the internal energy of that cell to simulate the energy release in the LVD reaction zone. The energy was added in three equal amounts over three calculational cycles (the time between successive cycles in the computation was about

0.35 μsec) since a detonation due to hot-spot initiation of collapsing bubbles is not expected to occur instantaneously throughout one region of the liquid. Since there is uncertainty as to the amount of energy actually released (specifically there is evidence that only a fraction of the heat of reaction is released during LVD), calculations were made using three different amounts of energy (EDET) to be added to each cell, in order to assess the effect of fractional energy release upon the overpressure and propagation speed of the LVD wave. The heat of reaction of ethyl nitrate which is approximately 5×10^9 ergs/gm, was used as the basis of EDET. A recompression of cavitated zones to the value of 0.4 kbar was chosen as the compression threshold for the initiation of reaction so that the low-amplitude compressional waves due to ringing behind the initial wall shock would not predetonate the liquid. This feature, in connection with the stress history in the liquid, is discussed in more detail below.

Results of LVD Computations

The important events that occur after impact are shown in Figure 2 for three simulations in which the EDET equaled 5×10^8 ergs/gm, 2×10^9 ergs/gm, and 5×10^9 ergs/gm or, respectively approximately 0.1, 0.4, and 1.0 times the heat of reaction of ethyl nitrate. The initial stress wave in the pipe wall, which travels at approximately 5.3 mm/μsec, quickly outdistances that in the liquid which travels at approximately 1.8 mm/μsec. When the former sufficiently outdistances the latter, or at approximately 0.7 I.D. down the pipe, the following sequence of events takes place. The compressive triaxial stresses in the pipe wall cause a small compressional wave to propagate into the liquid toward the center of the pipe and at the same time cause the pipe wall to expand radially. With this increase in radial strain, the hoop

stress in the pipe wall goes into tension and a tensile pulse is sent into the liquid shortly behind the initial compressive pulse. As this tensile pulse proceeds toward the center of the pipe, the liquid begins to cavitate, first at the cell near the pipe wall and finally at the central cell. Eventually the main compressive stress wave in the liquid reaches the cavitated zones and recompresses the liquid to above 0.4 kbar, which triggers the detonation. Since cavitation occurs earlier in the liquid cells near the edge of the pipe than in the cells at the center, and since the main compressional wave in the liquid reaches all of the cells at one axial position at about the same time, detonation begins earliest in the cell adjacent to the wall (at about 0.7 I.D. down the pipe) and latest at the center cell (at about 1.2 I.D.). This result is consistent with the observations of LVD in nitroglycerine reported by Sosnova et al.[19] that the most intense reaction is initiated in the nitroglycerine adjacent to the container wall and that the reaction wave profile is concave with respect to the direction of propagation in the initiating region. It should be noted, however, that since the inward-moving tensile pulses converge along the center line, the tensile stress is highest there and therefore the liquid in the center might be more highly cavitated. It is thus possible that under some conditions, perhaps when the initiating shock is relatively weak, LVD might occur primarily along the central region.

Figures 3a and 3b depict the computed stress histories at the central cell and at the cell adjacent to the pipe wall, respectively, for various distances down the tube in the case for which EDET = 5×10^8 ergs/gm. For each stress history there is initially a relatively small compressive pulse followed by a region of tension where the tensile stress is about 0.02 kbar. These wall-induced precursor waves are followed eventually by the main liquid compressive wave which triggers

the detonation. Note that for distances down the pipe greater than about 2.5 diameters, there are one or more additional cycles of precursor-induced compression and tension in the liquid prior to the arrival of the main liquid wave. These waves are due to the further ringing of the pipe following the initial compressional wave. If the compressional pulses following the initial cavitation, but prior to the arrival of the main liquid compression wave, were strong enough to collapse the voids and cause detonation, then the LVD wave would be coupled directly to the pipe wall wave and would travel at approximately the wave velocity in the pipe rather than at a velocity nearly that of the liquid shock. Since it is known experimentally that this does not happen, detonation was not triggered until the main liquid shock arrived. A detonation threshold of 0.4 kbar was chosen, which in the cases investigated is higher than the magnitude of the pressure in the liquid caused by ringing of the pipe wall.

Figures 4a and 4b depict, respectively, the computed axial and circumferential (hoop) stresses in the pipe at two distances down the tube for the same computation as above. The axial stress history of Figure 4a clearly shows the initial wall shock traveling at a speed of about 5.3 mm/μsec followed by a more gradual stress release and ringing. The hoop stress shown in Figure 4b rings back and forth between compression and tension following the initial pipe wave until a strong tension is produced by the detonation of the liquid inside the pipe.

Figure 5 shows the stress-strain loading and unloading curves of the liquid cell located at the center of the pipe 1.2 diameters down the pipe from the impacted end. The effects of the cavitation and detonation parameters used in the computations can be seen by comparing the two cases in which the liquid does and does not undergo cavitation and detonation.

The simulations in which EDET of 2×10^9 and 5×10^9 ergs/gm were used resulted in stress histories similar to those depicted in Figures 3 and 4. The two principal differences were that the LVD propagated at a slightly higher velocity--2.36 and 2.99 mm/μsec, respectively, than the 1.84 mm/μsec for the run using the lower EDET, and the pressure induced in the liquid by the LVD was significantly higher. Figure 6 contains stress histories at the central cell located 1.2 diameters down the pipe for all three simulations using the different values of EDET as well as the stress history for a simulation in which no detonation was allowed to take place. The simulation represented by these calculations closely approximates LVD in ethyl nitrate contained in a 1-inch I.D. by 1/8-inch wall steel pipe. Since measured LVD velocities for this system are on the order of 1.9 mm/μsec, the above results indicate that partial energy release is likely in LVD. This hypothesis is further substantiated by thermodynamic calculations of LVD which also indicate that partial energy release is likely.[20]

An additional computer simulation was made using lead as the pipe wall material. The stress wave velocity in the lead was only slightly higher (2.1 mm/μsec) than that in the liquid for the particular geometry and pressures of the simulation. The result was that the wall wave never quite ran far enough ahead of the liquid wave to cause any zone of tension in the liquid; therefore, no cavitation occurred to initiate LVD. Computations using different lead pipe wall thicknesses and stronger initiating shocks could conceivably result in precursor cavitation and an oscillating LVD wave. However, further computations of this type were beyond the scope of the current work.

Model for Cavitating Liquid

The model for cavitation used in these computations, in which the liquid simply expands at constant pressure when the tensile pressure exceeds 0.02 kbar and then subsequently contracts at constant pressure until the strain corresponds to that at 0.02 kbar in tension, is only a qualitative approximation of the cavitation behavior of a liquid undergoing tension. The more detailed phenomena of cavitation in a liquid undergoing dynamic tensile failure in the kilobar stress region have been discussed by Erlich et al.[21] A computer model of the dynamic equation of state of a cavitating liquid was developed which calculated growth and collapse of bubbles in a liquid strained at high rates. This model, which uses a viscous growth law and calculates the void volume and resulting stress relaxation for a given tensile strain, could be inserted in the FIBROUS code to describe more quantitatively the cavitation and subsequent bubble collapse for each liquid cell in the LVD simulation. The only unknown parameter in such a calculation would be the void nucleation frequency or the initial void volume, which can either be determined to sufficient accuracy for a given material by experiments of the type described in Reference 21 or by an approximation based on data for other liquids. When a liquid is subjected to tensile strain, rapid stress release occurs due to the nucleation and growth of c: ation bubbles. Thus, rather than using the strain at constant negative stress to simulate the cavitation behavior as was done here, a more realistic model would include dynamic bubble growth and the resulting stress release. In addition, once a zone of the liquid has been cavitated, a modified equation of state to include the dynamic bubble motion could be used. Computations using these improvements would give a more realistic picture of the cavitation and void collapse phenomena and could thus greatly improve the cavitation model of LVD.

Discussion

The axisymmetric computer calculations to simulate LVD in a cylindrical geometry show clearly the manner in which the container wall-liquid interaction produces zones of tension leading to cavitation of the liquid. Tension is produced in the liquid by waves propagating from the container walls into the liquid. The waves propagate into the liquid from the container walls much like Mach waves and converge at the tube centerline. If one computes the Mach angle, approximately equal to $\sin^{-1}(V_e/V_w)$, where $V_e \cong 1.8$ mm/μsec is the propagation speed of the wall waves and $V_w \cong 5.3$ mm/μsec is the wave propagation speed in the liquid, a value of approximately 20^o is obtained for the present system. This indicates that the time delay for precursor waves to propagate from the tube wall to the center cell should be about 5.3 μsec, a result that is consistent with that obtained by comparison of the precursor waves in Figures 3a and 3b. Thus, the cavitation produced by the precursor wall waves is a complex phenomenon that clearly cannot be accounted for by a one-dimensional analysis.

The recompression of a cavitated zone by the primary liquid shock is assumed to initiate hot-spot reactions, and the subsequent energy release--simulated by dumping an amount of energy EDET into the recompressed zone--drives the primary liquid shock. As can be seen by a comparison of Figures 3a and 3b, once the detonation is fully developed the liquid shock is approximately planar. Thus, even though the liquid next to the wall is cavitated prior to that in the center of the liquid, recompression occurs almost simultaneously over the tube cross section once the liquid shock is more than 1 or 2 diameters from the initiation end. Without detailed calculation of the bubble dynamics and appropriate modification of the liquid constitutive equations, the detailed effects of the time history upon the cavitation field cannot be fully explained.

During the initiation phase, which occurs approximately within the first two diameters from the donor end of the charge, the liquid shock is close enough bebind the wall shock to be within the Mach wave structure causing cavitation. Thus, reaction takes place only in the vicinity of the wall, the region where initiation was observed by Sosnova et al.[19] Watson et al.[11] observed a reaction zone in the region downstream of the initiation region where cavitation is generated across the entire tube cross section before arrival of the liquid shock.

The ringing of the tube wall behind the initial wall shock causes alternating zones of tension and compression in the liquid ahead of the main liquid shock (see Figure 3). The period of the oscillations is about 16 μsec for the present configuration. Studies of liquid failure, or cavitation at high stress rates,[21] show that significant bubble growth and the accompanying stress release can occur in less than 1 μsec for stresses on the order of those observed here. It is therefore likely that the ringing stresses produce significant bubble motion perhaps capable of collapsing the cavitation produced by the initial tension wave. Since experimental observations show that the reaction zone is not directly coupled to and does not move with the initial wall shock, as would occur if the ringing compressions caused bubble collapse and hot-spot initiation, the artifice was adopted here that a compression greater than 0.4 kbar was required to cause initiation. This effectively permitted hot-spot initiation at a precavitated zone only upon arrival of the main liquid shock. If, as seems likely, ringing of the liquid in the tube ahead of the main liquid shock is strong enough to collapse the bubbles but not strong enough to cause hot-spot initiation, then the main liquid shock will travel into alternating regions of cavitated and uncontacted liquid. This is a very possible explanation for the pulsating type of LVD, in which the detonation travels a short distance, this dies out, then begins again farther down the tube, and so forth.

That the recompression due to wall ringing does not cause initiation may be due to several reasons. First, the threshold stress for hot-spot initiation by a given bubble field is not known. It is therefore possible that the compression due to ringing is not strong enough to cause initiation. On the other hand, the equation of state of the cavitated liquid is only approximated in the present calculations and a more detailed model of the cavitation zone might provide a much different stress in the liquid due to the wall ringing. For example, the recompression by the final ringing wave following the first tension zone would be propagating into a dynamically cavitating liquid. Dispersive effects on the wave propagation caused by the bubble field could significantly alter the stress pattern from that computed here. The inclusion of a more detailed equation of state for the cavitated liquid which accounts for the dynamic bubble motions would represent a considerable extension of the current calculations and is currently being considered as a subject for further study.

As noted previously, if the LVD is to be truly a steady-state phenomenon, the wall wave caused by the detonation itself must be capable of causing precursor cavitation independently of the wall wave caused by the initial shock. (A quasi-steady state LVD, however, could occur for a considerable distance down a pipe if the cavitation bubbles remained in the liquid long after the ringing due to the initial wall shock had disappeared.) In the present calculations there is no indication that this is the case. One calculation was extended to an axial distance of $Z/D = 15$ and, even in the most energetic case (EDET = 5×10^9 ergs/gm) in which the shock pressure was in excess of 10 kbar, detonation-wave-coupled precursor wall waves capable of causing cavitation directly ahead of the liquid shock were not observed. Thus, while not conclusive, the work here indicates that cavitation is caused only by the precursor wall wave generated by the initiating shock.

Conclusions

The computations described above support the cavitation model for the initiation and propagation of LVD and provide a first step towards a detailed quantitative description of these processes. The results support the hypothesis that only partial energy release occurs in LVD. There is no indication that the wall wave caused by the detonation itself produces zones of tension capable of producing cavitation. However, further conclusions regarding these results must await additional calculations for different geometries, different materials, and more accurate modeling of the equation of state of the cavitated liquid.

REFERENCES

1. A. Stettbacker, "Zünding und Detonation," Z. ges. Schiess-Sprengstoffe, 14, 137 (1919).

2. A. A. Deserhkovich and K. K. Andreev, "Über Die Eigenschaften der Nitroglycerine-Isomeren," Z. ges., Schiess-Sprengstoffe, 25, 353 (1930).

3. L. G. Bolkhovitinov, "The Low Velocity Detonations of Liquid Explosives," Dok. Acad. Nauk, 130 (5), 1046 (1960).

4. F. P. Bowden and O. A. Gurton, "Birth and Growth of Explosion in Liquids and Solids Initiated by Impact and Friction," Proc. Roy. Soc. A, 198, 350 (1949).

5. H. Eyring, R. E. Powell, G. H. Duffey, and R. B. Parlin, "Stability of Detonation," Chem. Rev., 45, 96 (1949).

6. M. W. Evans, "Detonation Sensitivity and Failure Diameter in Homogeneous Condensed Materials," J. Chem. Phys. 36, 193 (1962).

7. R. Schall, "Die Stabilitaet Langsamer Detonation," Z. Angew. Phys. VI Band, 10, 470 (1954).

8. R. W. Woolfolk and A. B. Amster, "Low Velocity Detonations: Some Experimental Studies and Their Interpretation," Twelfth Symposium (International) on Combustion, The Combustion Institute, Pittsburgh 1969, p. 731.

9. R. W. Watson, C. R. Summers, F. C. Gibson, and R. W. Van Dolah, "Detonations in Liquid Explosives--The Low Velocity Regime," Proceedings Fourth Symposium (International) on Detonation, Office of Naval Research, Department of the Navy, Washington, D.C. ACR-126, p. 117.

10. I. N. Voskoboinikov, A. V. Dubovik, and V. K. Bobolev, "Low Velocity Detonation in Nitroglycerine," Inst. Chem. Phys. Acad. Sci. USSR, Trans. from Dokl. Akad., Nauk, 161 (5), 1152 (1965).

11. R. W. Watson, "The Structure of Low-Velocity Detonation Waves," Twelfth Symposium (International) on Combustion, The Combustion Institute, Pittsburgh, 1969, p. 723.

12. R. W. Watson, J. Ribovich, J. E. Hay, and R. W. Van Dolah, "The Stability of Low-Velocity Detonation Waves," Fifth Symposium (International) on Detonation, ONR Report DR 163, 71 (1970).

13. F. C. Gibson, R. W. Watson, J. E. Hay, C. R. Summers, J. Ribovich, and F. H. Scott, "Sensitivity of Propellant Systems," Quarterly Report, U.S. Dept. of Interior, Bureau of Mines, Pittsburgh, February 2, 1966.

14. F. C. Gibson, R. W. Watson, J. E. Hay, C. R. Summers, J. Ribovich, F. H. Scott, "Sensitivity of Propellant Systems," Quarterly Report, U. S. Department of Interior, Bureau of Mines, Pittsburgh, May 19, 1966.

15. "Card Gap Test for Shock Sensitivity of Liquid Monopropellants," Liquid Propellant Test Methods, Liquid Propellant Information Agency, Applied Physics Laboratory, Johns Hopkins University, Silver Spring, Maryland (1960).

16. M. L. Wilkins, "Calculations of Elastic-Plastic Flow," Methods of Computational Physics, Vol. III, Fundamental Methods in Hydrodynamics, p. 211, Eds. B. Alder, S. Fernbeck, M. Rottenberg, Academic Press, New York (1964).

17. M. H. Rice, R. G. McQueen, and J. M. Walsh, "Compression of Solids by Strong Shock Waves," Solid State Physics Vol. 6 (Academic Press, 1958) p. 41, Eds. F. Seitz and D. Turnbull.

18. J. W. Taylor and M. H. Rice, "Elastic-Plastic Properties of Iron," J. Appl. Phys. 34, 364 (1963).

19. G. S. Sosnova, I. M. Voskoboinikov, and A. V. Dubovik, "Light Emitted by a Detonation Front of Low Velocity in Nitroglycerine," Dokl. Akad. Nauk, SSSR, 149, 642 (1963).

20. M. Cowperthwaite, "Hydrothermodynamics of the Cavitation Model of Low Velocity Detonation," Appendix B of this report.

21. D. C. Erlich, D. C. Wooten, and R. C. Crewdson, "Dynamic Tensile Failure of Glycerol," J. Appl. Phys. 42 (1971).

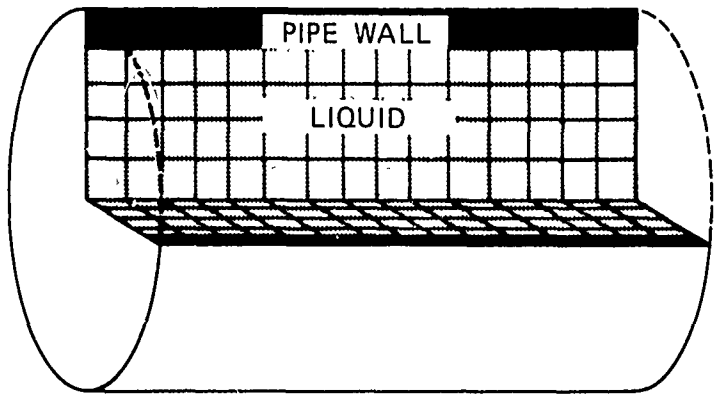

GA-7771-1A

FIGURE A-1 RECTANGULAR GRID REPRESENTATION OF LIQUID-FILLED PIPE USED IN FIBROUS COMPUTER CODE

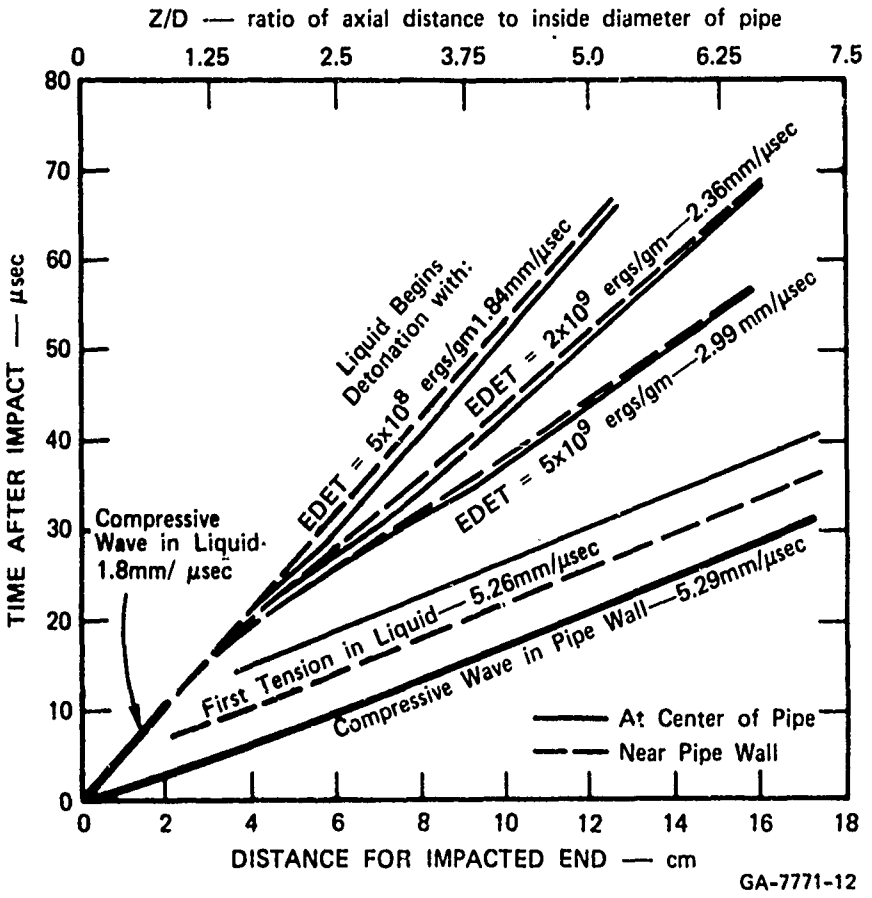

FIGURE A-2 WAVE DIAGRAM SHOWING RELEVANT EVENTS IN LVD COMPUTER SIMULATION

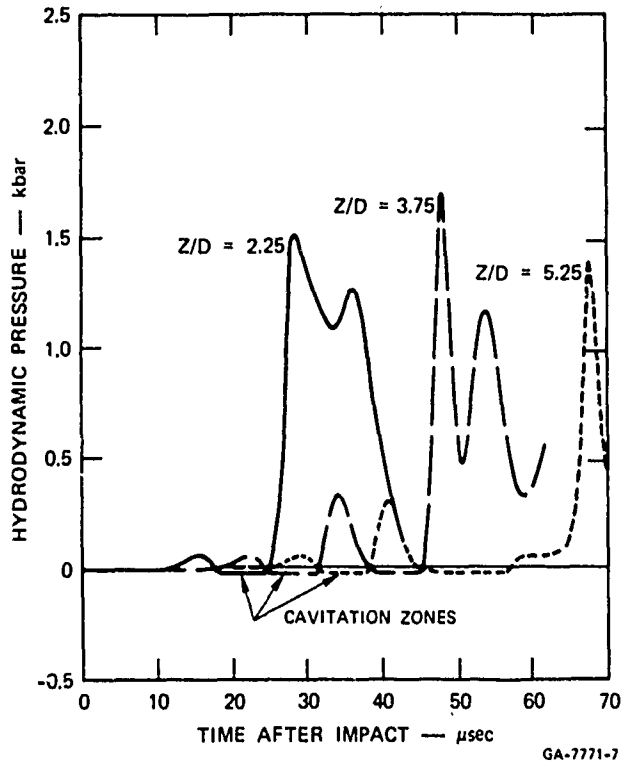

(a) IN THE CENTER OF THE PIPE

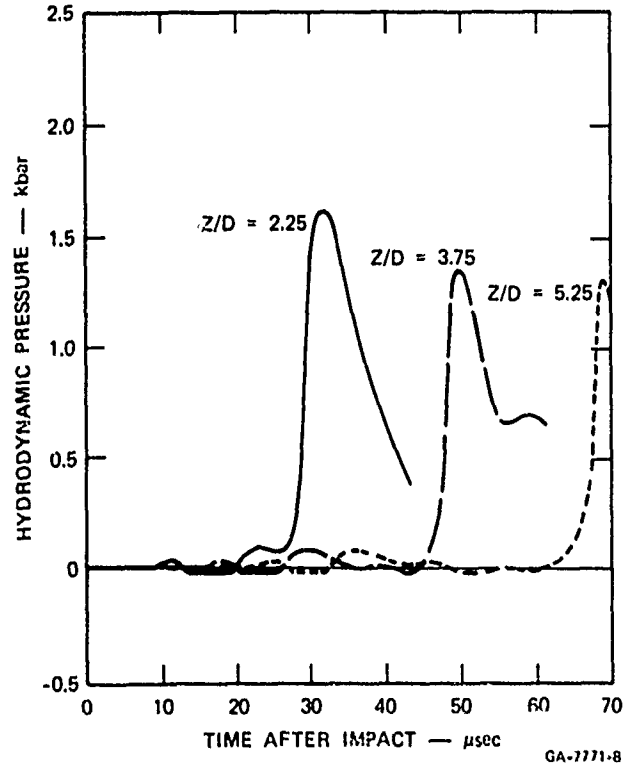

(b) ADJACENT TO THE PIPE WALL

FIGURE A-3 COMPUTED LIQUID PRESSURE HISTORIES FOR RUN IN WHICH EDET = 5 x 10^3 ergs/gm AT CELL LOCATIONS

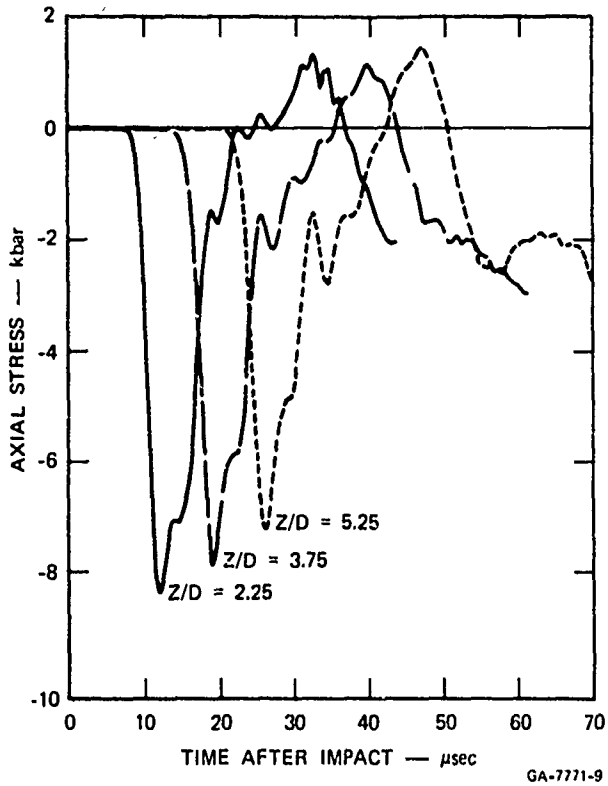

(a) AXIAL

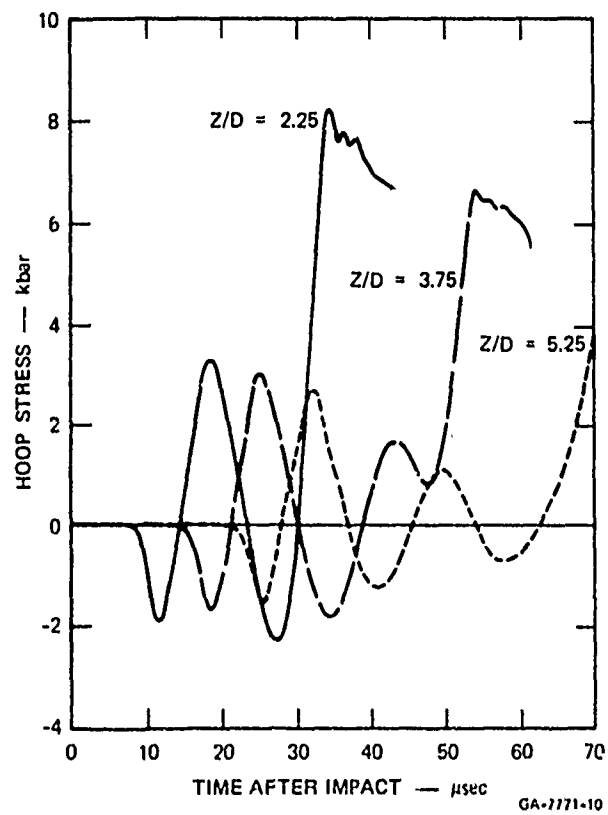

(b) CIRCUMFERENTIAL STRESS HISTORIES IN THE PIPE WALL AT SEVERAL LOCATIONS FOR THE SIMULATION IN WHICH EDET = 5×10^8 ergs/gm

FIGURE A-4 AXIAL (a) and CIRCUMFERENTIAL (b) STRESS HISTORIES IN THE PIPE WALL AT SEVERAL LOCATIONS FOR THE SIMULATION IN WHICH EDET = 5×10^8 ergs/gm

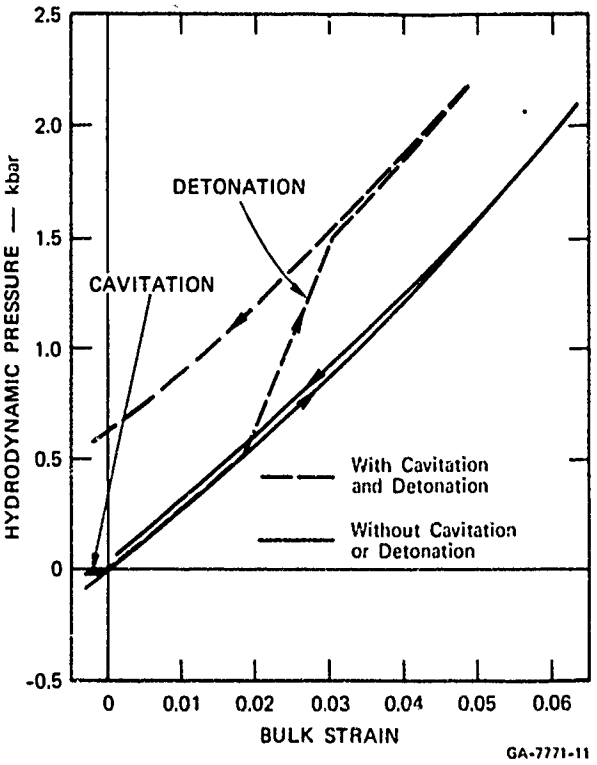

FIGURE A-5 STRESS-STRAIN LOADING AND UNLOADING CURVE FOR THE LIQUID IN THE LVD COMPUTER SIMULATION SHOWING EFFECTS OF CAVITATION AND DETONATION MODELS USED

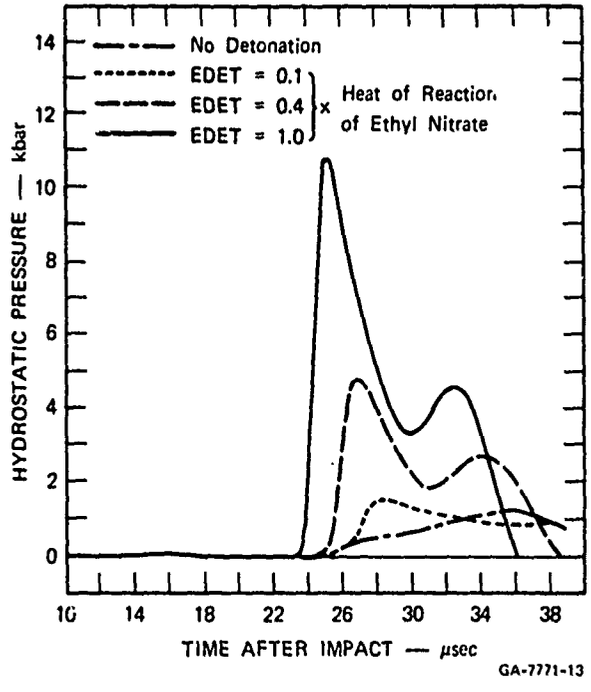

FIGURE A-6 PRESSURE HISTORIES OF THE LIQUID CELL IN THE CENTER OF THE PIPE AT A DISTANCE OF 1.2 INSIDE DIAMETERS FROM THE IMPACTED END FOR DIFFERENT VALUES OF EDET (EDET FOR ETHYL NITRATE ≅ 5 X 10^9 ergs/gm)

Appendix B

HYDROTHERMODYNAMICS OF THE CAVITATION MODEL FOR LOW VELOCITY DETONATION

HYDROTHERMODYNAMICS OF THE CAVITATION MODEL FOR LOW VELOCITY DETONATION*

By

M. Cowperthwaite
Physical Sciences Division
Stanford Research Institute
Menlo Park, California

*This work was supported by the U.S. Air Force Office of Scientific Research under Contract No. F44620-69-C-0079.

47

Introduction

Shock wave studies during the last decade,[1-6] extending earlier work discussed in the book by Taylor,[7] have established that many liquid propellants and explosives exhibit two modes of self-sustaining detonation. These modes have distinct velocities of propagation and have been characterized accordingly as high-velocity detonation (HVD) and low-velocity detonation (LVD). The high-velocity mode propagates at approximately 6 mm/μsec with a pressure of about 100 kilobars; the low-velocity mode propagates with a slightly higher velocity than ambient soundspeed, at approximately 2 mm/μsec with a pressure of about 10 kilobars. The hydrodynamic theory of detonation, together with the Chapman-Jouguet (C-J)[8,9] hypothesis, provides a satisfactory model for calculating HVD velocities when the equation of state of the detonation products is known, but not for calculating LVD velocities at the present time.

The Cavitation Model for LVD

The present work is concerned with the problem of formulating a model for calculating the propagation velocity of LVD. It is based on the physical model proposed by workers at the Bureau of Mines after an extensive experimental investigation of LVD. This model was discussed by Watson[5] at the Twelfth International Symposium on Combustion. LVD is modeled as a reactive shock propagating in a cavitated liquid. The cavitation field ahead of the shock is produced by interactions between the liquid and container wall; the reaction required to support the wave is initiated in bubbles compressed by the shock. This model is called the cavitation model of LVD.

Propagation of LVD is thus a very complex phenomenon involving the formation of a cavitation field and its subsequent behavior under shock compression. A detailed treatment must account for liquid-container wall interactions and also for the dynamics and thermodynamics of a cavitation field with heat transfer, mass transfer, and chemical reaction. Here, however, it is assumed that a detailed account of these processes is not required to calculate the propagation velocity of LVD. The processes will be modeled simply with well-defined assumptions related to their characteristic times. This approach is motivated by the one-dimensional C-J model for gaseous detonation, which is satisfactory for calculating the average velocity of self-sustaining detonation waves without treating the complex system of interacting transverse waves necessary for their propagation. As with the C-J model, the validity of assumptions and the model based upon them must be determined by the comparison of calculated LVD propagation velocities with those obtained experimentally.

Hydrothermodynamic Assumptions

Our one-dimensional treatment of LVD is based on the following assumptions ordering the time scales for cavitation, mechanical equilibrium, and chemical reaction. The cavitation field is assumed to be formed quickly ahead of the main shock in the liquid, and under shock compression is assumed to attain mechanical equilibrium and form a steady-state burning zone. The implications of the assumptions are as follows. The rapid formation of the cavitation field necessitates that the shock in the liquid be represented by a Rayleigh line[8] passing through the initial state of the cavitated liquid and not the initial state of the virgin liquid. The assumption about mechanical equilibrium implies that pressure be well defined at each point of the reaction

zone, and specifies the initial state for burning as the initial shocked state produced in the cavitated liquid. The steady-state assumption leads to the conclusion that the reaction zone lies on the Rayleigh line representing the main shock in the cavitated liquid. An additional assumption about the termination of the reaction zone is required to formulate a model for calculating the propagation velocity of LVD. We will first consider the case when the reaction attains equilibrium at the termination of the steady state and then the case when it does not.

Complete Equilibrium

Considerations based on the properties of Hugoniot curves lead to the conclusion that the cavitation model for LVD gives a unique propagation velocity when the reaction zone ends in a state of complete equilibrium. The Hugoniot for cavitated liquid is shown schematically in the pressure-specific volume (p-v) plane as OSH in Figure 1*; the detonation branch of the equilibrium products Hugoniot curve[8,9] centered at O is shown as $O'JH'$ and the Rayleigh line tangent at its C-J point J as OJS. The point of intersection of the Rayleigh line Oi passing through the initial condition O, with slope $-(D/v_o)^2$, and OSH represents the initial shocked state i produced by a shock propagating at velocity D in the cavitated liquid with initial volume v_o. Since the initial state for burning is the initial shocked state, the final burnt state must lie on the deflagration branch of an equilibrium products Hugoniot centered on OSH. We are therefore interested in the deflagration branches of the family of equilibrium products Hugoniot curves centered on OSH

For convenience, we will consider the family of deflagration Hugoniot curves centered on OSH above S with $p_i > p_s$. A member of this family is shown schematically in Figure 1 as $O_iJ'O_i'$. When $p_i > p_s$, we will

* Figures are shown at the end of this appendix.

show that the points of intersection of the Rayleigh line Oi with the detonation branch of the products Hugoniot curve centered at the initial condition O lie on the deflagration branch of the products Hugoniot curve centered at i. The points of intersection of Oi and O′JH′ are shown in Figure 1 as 1 and 2. It is convenient first to relate the states O, i, and 2 by expressing the conditions that i and 2 lie on the Hugoniot curves centered at O and also on the Rayleigh line O2i. Let e denote specific internal energy, then (e, p, v) states on a Hugoniot curve are related by the Hugoniot equation[8] expressing the balance of mass, momentum, and energy across a shock discontinuity. The Hugoniot equation for a Hugoniot curve centered at $O(e_o, p_o, v_o)$ is

$$2(e - e_o) = (p + p_o)(v_o - v) \qquad (1)$$

and the conditions for i to be on OSH and 2 to be on O′JH′ follow from Eq. (1) as

$$2(e_i - e_o) = (p_i + p_o)(v_o - v_i) \qquad (2)$$

$$2(e_2 - e_o) = (p_2 + p_o)(v_o - v_2) \qquad (3)$$

The condition for these states to be on the Rayleigh line Oi follows from the Rankine-Hugoniot jump conditions[8] as

$$\frac{p_2 - p_o}{v_o - v_2} = \frac{p_i - p_o}{v_o - v_i} \; . \qquad (4)$$

The combination of Eqs. (2), (3), and (4) to eliminate e_o, p_o, and v_o leads to the equation

$$2(e_2 - e_i) = (p_2 + p_i)(v_i - v_2) \qquad (5)$$

relating the states i and 2, and a similar argument leads to the equation

$$2(e_1 - e_i) = (p_1 + p_i)(v_i - v_1) \qquad (6)$$

relating the states i and 1. Equations (5) and (6) show that states 2 and 1 satisfy the Hugoniot equation

$$2(e - e_i) = (p + p_i)(v_i - v) \qquad (7)$$

for the deflagration branch of the products Hugoniot $O_i J' O_i'$ centered at i. Thus when $p_i > p_s$, the deflagration branch of the products Hugoniot centered at i and the detonation branch of the products Hugoniot centered at O intersect at the points where the Rayleigh line connecting O and i intersects the detonation branch centered at O.

It is clear from Figure 1 that the intersection points 1 and 2 approach each other as p_i approaches p_s and coincide at J when $p_i = p_s$. Moreover, when $p_i > p_s$ the Rayleigh line iJ' tangent to $O_i J' O_i'$ intersects the $p = 0$ axis at a point to the left of the initial condition O. When $p_i < p_s$, the deflagration branch of the Hugoniot centered at i does not intersect the detonation branch of the Hugoniot centered at i, and its tangent Rayleigh line intersects the $p = 0$ axis at a point lying to the right of O. A unique situation arises when $p_i = p_s$, for then the Hugoniots centered at O and i are tangent to the Rayleigh line OS at J, and the C-J points of both curves coincide. This condition is the only one compatible with our assumption of a steady state terminating in complete equilibrium because in this case the Rayleigh line must be tangent to the deflagration branch of the Hugoniot centered on the initial shocked state and must also pass through the initial state of the cavitated liquid.

Thus conditions for a steady state define a unique propagation velocity in the simplest case when the reaction attains equilibrium. The propagation velocity for LVD with the reaction attaining equilibrium in the cavitation model is determined by the C-J condition on the detonation branch of the equilibrium Hugoniot centered on the cavitated liquid.

To test the model with a realistic equation of state, the TIGER code developed at Stanford Research Institute for the Ballistic Research Laboratories under Contract No. DA-04-200-AMC-3226(X), was used to calculate the detonation parameters of ethyl nitrate for different degrees of cavitation. The internal energy of the cavitated liquid ahead of the shock was assumed to be the same as that of the uncavitated liquid. The results of these calculations are shown in Table 1. Calculations with the BKW and the virial equation of state do not agree with experiment, even when the volume of the cavitated liquid greatly exceeds that expected experimentally. Propagation velocities calculated with the ideal gas equation of state agree with experiment, but the detonation pressures lie in the kilobar region where this equation of state is inapplicable.

The results of these calculations lead to the conclusion that the assumption of complete reaction is not valid. Attention was therefore given to a study of the cavitation model when the reaction does not attain equilibrium.

Incomplete Equilibrium

We will use a reaction coordinate λ to denote the fraction of unburnt liquid when the reaction does not attain equilibrium. Then $\lambda = 0$ in the former case when the reaction attains equilibrium and all the liquid is consumed, and $\lambda = 1$ when there is no reaction. Our treatment of partial equilibrium is based on the assumption that the

reaction is frozen with the products in chemical equilibrium. In this case a value of λ defines an equilibrium products Hugoniot curve for incomplete reaction--a frozen Hugoniot--centered on the initial condition of the cavitated liquid. And the values of λ in the range $0 < \lambda < 1$ define a family of frozen Hugoniot curves lying between the Hugoniot curve of the cavitated liquid and the equilibrium products Hugoniot for complete reaction.

It follows from the previous treatment of complete equilibrium that LVD will be represented by a Rayleigh line tangent to the detonation branch of a frozen Hugoniot centered on the initial state 0 of the cavitated liquid. An equation of state for nitromethane was incorporated into the TIGER code so that detonation parameters could be calculated with a realistic thermodynamic description of the explosive and the products of reaction. Detonation parameters were calculated as a function of λ to determine if LVD could be modeled with the cavitation model.

A complete equation of state[10] of the liquid explosive must be incorporated into the TIGER code to compute detonation parameters when the reaction does not proceed to equilibrium. A knowledge of the incomplete pressure-volume-temperature (p-v-T) equation of state and the variation of specific heat at constant pressure C_p along the atmospheric isobar is required to introduce a complete equation of state into the TIGER code. The thermodynamic functions required to compute a thermodynamic state are calculated by integrating thermodynamic identities along isotherms from the atmospheric isobar. The (p-v-T) relationship used in the present work was based on the equation of state for liquids[11] formulated previously for shock temperature calculations. In this description of liquids, $(\partial p/\partial T)_v$ is assumed to be constant and the specific heat at constant volume C_v is assumed to be a function of temperature, i.e. $C_v(T)$. Nitromethane was chosen as a typical liquid

explosive because $C_v(T)$ and the shock temperature along the Hugoniot curve were known from the previous work.[11] The standard Hugoniot centered on the initial state (p_o = 1 atmosphere, $T_o = 298^oK$, and $v_o = 0.884$ cc/g) in the (p-v) plane was constructed with the universal Hugoniot for liquids $U = a_1 c_o + a_2 u$ where a_1 and a_2 are constants; and U, u, and c_o denote shock velocity, particle velocity, and sound speed in the initial condition.*

Let $b = (\partial p/\partial T)_v$, $\alpha = 1/v_o(\partial v/\partial T)_{p=1}$ and let the subscript h denote states on the standard Hugoniot curve shown schematically as 03h in Figure 2. The (p-v-T) equation of state in the region $v \leq v_o$ spanned by the Hugoniot curve can be written as

$$p = p_h(v) + b[T - T_h(v)], \quad v \leq v_o \tag{8}$$

where

$$p_h(v) = p_o + (a_1 c_o)^2 (v_o - v_h)/[v_o - a_2(v_o - v_h]^2 \tag{9}$$

and $T_h(v)$ is calculated by integrating the differential equation governing temperature along the Hugoniot curve. The (p-v-T) equation of state was extended to the right of v_o by assuming that $(\partial v/\partial T)_p$ was constant and therefore equal to αv_o along the atmospheric isobar $p = p_o = 1$ when $v \geq v_o$. With this assumption the (p-v-T) equation of state in the region $v \geq v_o$ can be written as

$$p - p_o = b[(T - T_o) - 1/\alpha(v/v_o - 1)], \quad v \geq v_o . \tag{10}$$

---

*Additional work on the universal Hugoniot curve for liquids is presented in this report in Appendix C.

Equations (8) and (10) have continuous first derivatives where they are patched together along the v_o isochore 042. In performing an integration along an isotherm, say 543 (Fig. 2), Eq. (10) is used until $v = v_o$ at 4, and then Eq. (8) is used along 43 for $v \leq v_o$.

Equations for the specific Gibbs free energy G, the specific entropy S, the specific enthalpy H, and C_p were derived with Eqs. (8) and (10) and incorporated into the TIGER code. But only the equations for G will be given here because the equations for the other state variables can be calculated from them with thermodynamic identities. For $v \geq v_o$, the equation for G is

$$G(T,v) = G(T) - b/2\, \alpha v_o [v^2 - (v(T))^2] \qquad (11)$$

with

$$G(T) = G_o - S_o(T - T_o) - T \int_{T_o}^{T} (C_p/T)\, dT + \int_{T_o}^{T} C_p\, dT \qquad (12)$$

and

$$v(T) = v_o(1 + \alpha(T - T_o)) \,. \qquad (13)$$

For $v \leq v_o$, it is

$$G(T,v) = G(T,v_o) + pv - p(T,v_o)\, v_o - bT(v - v_o) - I_p + bI_T \qquad (14)$$

where $G(T,v_o)$ and $p(T,v_o)$ are obtained by setting $v = v_o$ in Eqs. (8) and (11), and $I_p = \int_{v_o}^{v} p_h dv$ and $I_T = \int_{v_o}^{v} T_h dv$ denote the integrals of shock pressure and temperature along the Hugoniot curve.

The SPECIAL routine, developed at Stanford Research Institute for Picatinny Arsenal under Contract DAAA21-71-C-0454 to treat nonideal detonation, was used to calculate detonation parameters of cavitated nitromethane as a function of the unreacted fraction λ with different equations of state for the reaction products. Most of the calculations

were performed with the virial equation of state because we are interested in detonation pressures in the region of 10 kilobars. The virial equation of state used in the TIGER code contains the second virial coefficient B and the third virial coefficient C. The results of the calculations performed without the third virial coefficient (C = 0) for a 10 percent increase in initial volume are given in Table 2, and the results of the calculations performed with the BKW and ideal gas equations of state, and the virial equation with $C \neq 0$ are also given. Because of convergence problems in the SPECIAL routine, the calculations for a 10 percent increase in initial volume were limited to values of λ in the range $0 < \lambda \leq 0.625$, and the case of a 20 percent increase in the initial volume was considered.

The results of the calculations performed for a 20 percent increase in initial volume using the virial equation with $C = 0$ are given in Table 3. The virial equation with $C = 0$ is used for all values of λ for convenience because the SPECIAL routine was formulated to calculate detonation parameters along the frozen C-J locus from the equilibrium, $\lambda = 0$, C-J state. The calculated detonation pressures and velocities for λ in the range $0 < \lambda \leq 0.75$ are plotted as a function of λ in Figure 3. For values of $\lambda > 0.75$ the graphs were extrapolated smoothly to satisfy the boundary conditions that the pressure approaches one atmosphere and the velocity approaches the sound speed in the cavitated liquid as λ approaches one. The sound speed in cavitated liquid was estimated to be 1.88 mm/μsec when the increase in initial volume was 10 percent and to be 1.08 mm/μsec when the increase was 20 percent.

It follows from Figure 3 that the calculations are not completely definitive because experimental values of LVD velocity and pressure correspond to values of $\lambda \approx 0.8$ and lie in the region where the results

of the calculations had to be extrapolated. Further examination of Figure 3, however, shows that the curves for a 10 and 20 percent increase in initial volume lie very close together in the 10-kilobar region and leads to the conclusion that a surprisingly small amount of reaction is required to support LVD. Important features of the cavitation model with incomplete reaction can therefore be stated as follows:

(1) Only reaction of about 20 percent of the liquid is required to support LVD.

(2) LVD parameters do not depend strongly on the initial degree of cavitation.

Conclusions

It is clear that additional work is required to formulate a satisfactory method for calculating the propagation velocity of LVD. This work should be concerned mainly with the degree of incomplete reaction. An attempt should be made to establish a condition for the termination of the reaction zone so that there is a unique propagation velocity for the cavitation model with incomplete reaction. A consideration of bubble dynamics with heat and mass transfer and chemical reaction should be undertaken to try and determine a criticality condition for termination of reaction and a means of calculating a value of λ at the end of the reaction zone. LVD velocities for different explosives calculated with values of λ could then be used to test the validity of the cavitation model. The detonation products of a liquid explosive undergoing first HVD and then LVD should be collected and compared to test if the amount of reaction predicted by the present work with the cavitation model for LVD is reasonable.

Acknowledgments

The author thanks D. C. Wooten, R. W. Woolfolk, and R. Shaw for helpful discussions, and is greatly indebted to W. Zwisler for incorporating the $C_v(T)$ equation of state for liquids into the TIGER code and calculating the detonation parameters with the SPECIAL routine.

REFERENCES

1. L. G. Bolkhovitinov, Dokl. Akad. Nauk 130, 1044 (1960).

2. I. M. Voskoboinikov, A. V. Dubovick, and V. K. Bobolev, Dokl. Akad. Nauk, SSSR, 161, 1152 (1965).

3. R. W. Watson, C. R. Summers, F. C. Gibson, and R. W. Van Dolah, Proceedings, Fourth Symposium (International) on Detonation ACR-126, Office of Naval Research, Department of the Navy, Washington, D.C., p. 117.

4. A. B. Amster, D. M. McEachern, Jr., and Z. Pressman, Proceedings, Fourth Symposium (International) on Detonation ACR-126, Office of Naval Research, Department of the Navy, Washington, D.C., p. 126.

5. R. W. Watson, Twelfth Symposium (International) on Combustion, The Combustion Institute, Pittsburgh, Pa., 1969, p. 723.

6. R. W. Woolfolk and A. B. Amster, The Twelfth Symposium (International) on Combustion, The Combustion Institute, Pittsburgh, 1969, p. 731.

7. J. Taylor, Detonation in Condensed Explosives, Chapter X, Oxford at the Clarendon Press 1952.

8. R. Courant and K. O. Friedrichs, Supersonic Flow and Shock Waves (Interscience, New York 1948).

9. Ya B. Zeldovich and A. S. Kompaneets, Theory of Detonation, Academic Press, New York and London, 1960.

10. M. Cowperthwaite and J. H. Blackburn, NBS Special Publication 326, Accurate Characterization of the High-Pressure Environment, p. 137.

11. M. Cowperthwaite and R. Shaw, J. Chem. Phys. 53, 555 (1970).

Table 1

DETONATION PARAMETERS IN ETHYL NITRATE CALCULATED WITH THE TIGER CODE

Equation of State	Initial Volume (cc/g)	Detonation Velocity (mm/μsec)	C-J Particle Velocity (mm/μsec)	C-J Pressure (kbar)	C-J Volume (cc/g)	C-J Temperature (^{o}K)
BKW	0.905*	6.73	1.81	132.8	0.66	2608
	1.77	4.80	1.48	39.6	1.23	2666
	2.03	4.56	1.43	31.7	1.39	2625
	2.37	4.31	1.37	24.6	1.61	2585
	2.82	4.04	1.31	18.53	1.91	2572
Virial**	0.905*	4.02	1.31	57.0	0.61	3277
	1.77	3.36	1.16	21.7	1.16	2981
	2.03	3.25	1.14	18.0	1.32	2930
	2.37	3.14	1.11	14.6	1.53	2878
	2.82	3.02	1.09	11.5	1.81	2827
Ideal Gas	0.905*	2.22	1.00	17.0	--	--
	1.77	2.22	1.00	12.2	0.98	2728
	2.03	2.22	1.00	10.6	1.12	2718
	2.37	2.22	1.00	9.1	1.31	2708
	2.82	2.22	1.00	7.6	1.56	2698

* Detonation in virgin material (no cavitation).

** Third virial coefficient set equal to zero.

6/

Table 2

CALCULATED DETONATION PARAMETERS FOR NITROMETHANE
WITH THE INITIAL VOLUME INCREASED TEN PERCENT

Equation of State	Unreacted Fraction (λ)	Detonation Velocity (mm/μsec)	C-J Pressure (atm. x 10^3)	C-J Volume (cc/g)	Adiabatic Index (χ)
Virial (C = 0)	0.0	4.04	54.9	0.650	2.02
	1/16	3.91	53.9	0.635	1.88
	1/8	3.79	51.4	0.629	1.83
	3/16	3.66	48.6	0.625	1.80
	1/4	3.53	45.6	0.623	1.78
	3/8	3.29	39.5	0.622	1.78
	1/2	3.05	33.7	0.625	1.80
	5/8	2.80	27.5	0.635	1.88
BKW	0.0	6.49	118.7	0.702	2.59
	1/4	5.55	81.9	0.717	2.82
	1/2	4.47	50.8	0.729	2.99
Virial (B and C)	0.0	5.20	79.5	0.691	2.45
	1/8	4.70	65.1	0.689	2.44
	1/4	4.24	53.7	0.685	2.39
	3/8	3.82	44.5	0.679	2.32
Ideal Gas	0.0	2.32	24.8	0.533	1.22
	1/4	2.62	33.6	0.503	1.07
	1/2	2.44	28.4	0.515	1.13

Table 3

CALCULATED DETONATION PARAMETERS FOR NITROMETHANE
WITH THE INITIAL VOLUME INCREASED 20 PERCENT

Equation of State	Unreacted Fraction	Detonation Velocity (mm μsec)	C-J Particle Velocity (mm/μsec)	C-J Pressure (cc/g)	C-J Volume (cc/g)	C-J Temperature (°K)	Adiabatic Index (κ)
Virial (C = 0)	0.0	3.93	1.32	47.8	0.711	3568	1.99
	1/8	3.74	1.43	49.3	0.661	3259	1.62
	1/4	3.49	1.36	43.8	0.654	2853	1.58
	3/8	3.25	1.26	37.9	0.653	2468	1.57
	1/2	3.00	1.16	32.2	0.656	2114	1.59
	5/8	2.75	1.04	26.3	0.666	1767	1.65
	3/4	2.43	0.85	19.1	0.695	1364	1.86

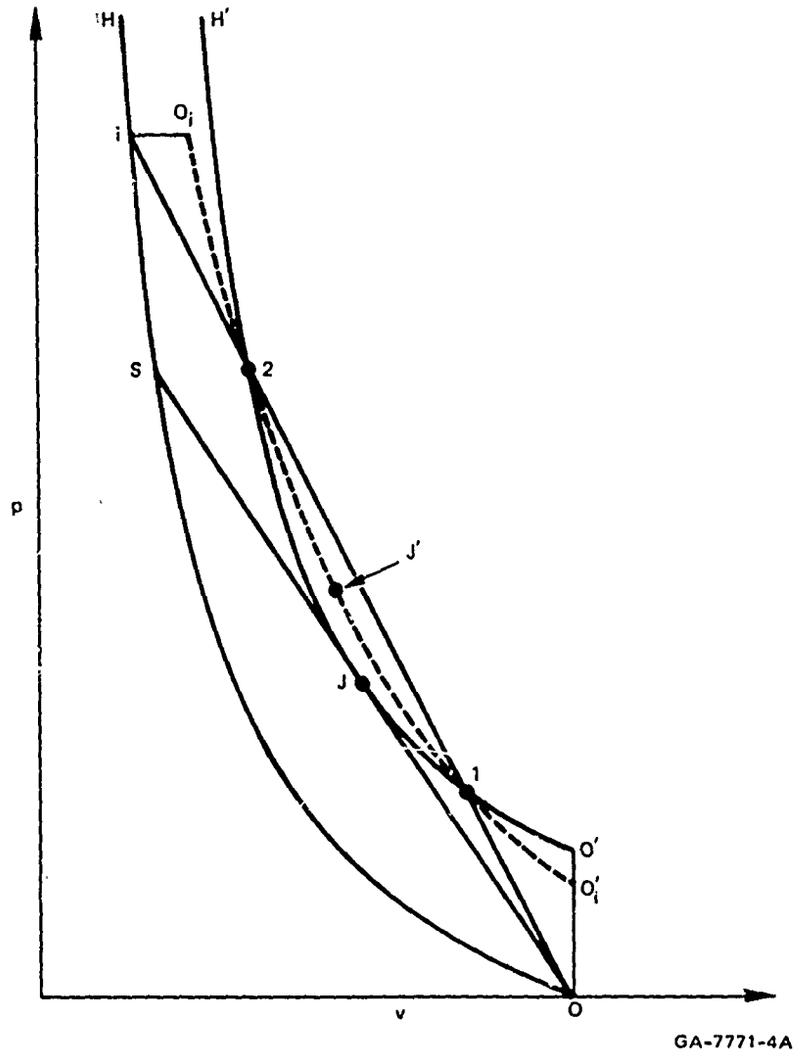

FIGURE B-1 SCHEMATIC DIAGRAM OF HUGONIOT CURVES IN THE (p-v) PLANE

64

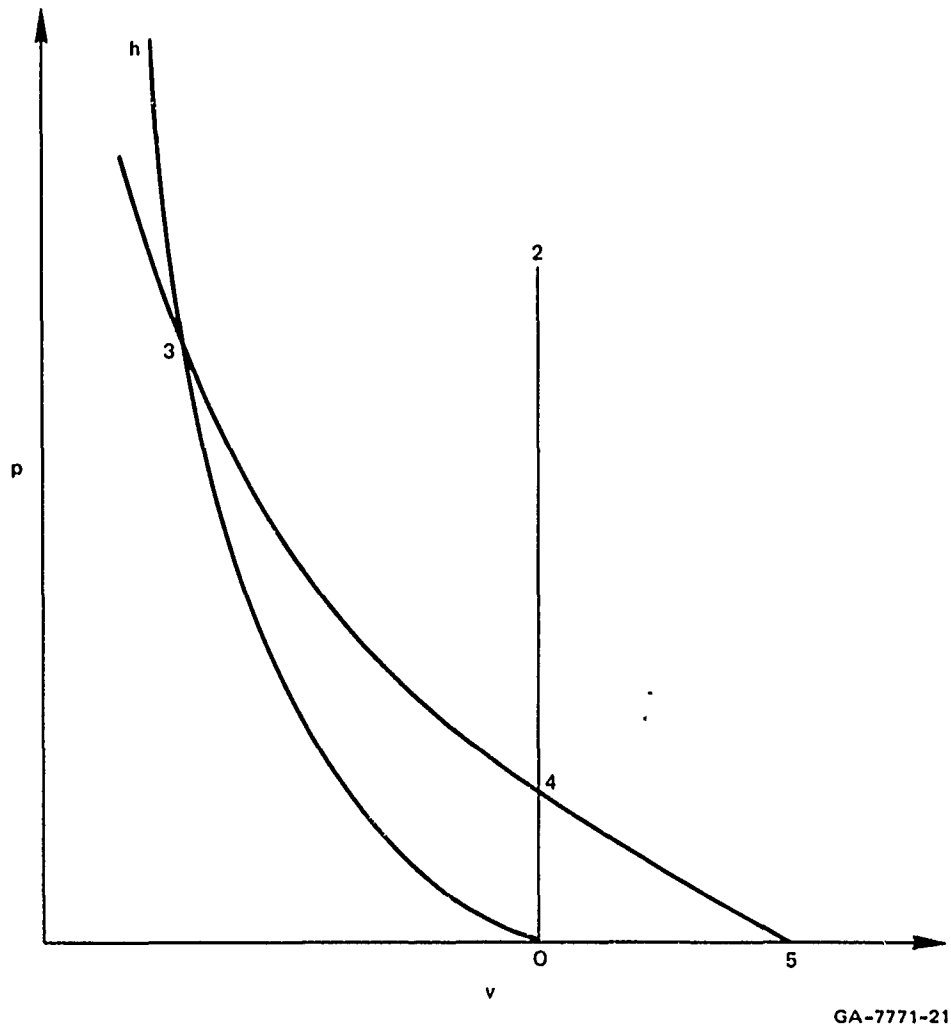

FIGURE B-2 SCHEMATIC HUGONIOT AND ISOTHERM FOR NITROMETHANE

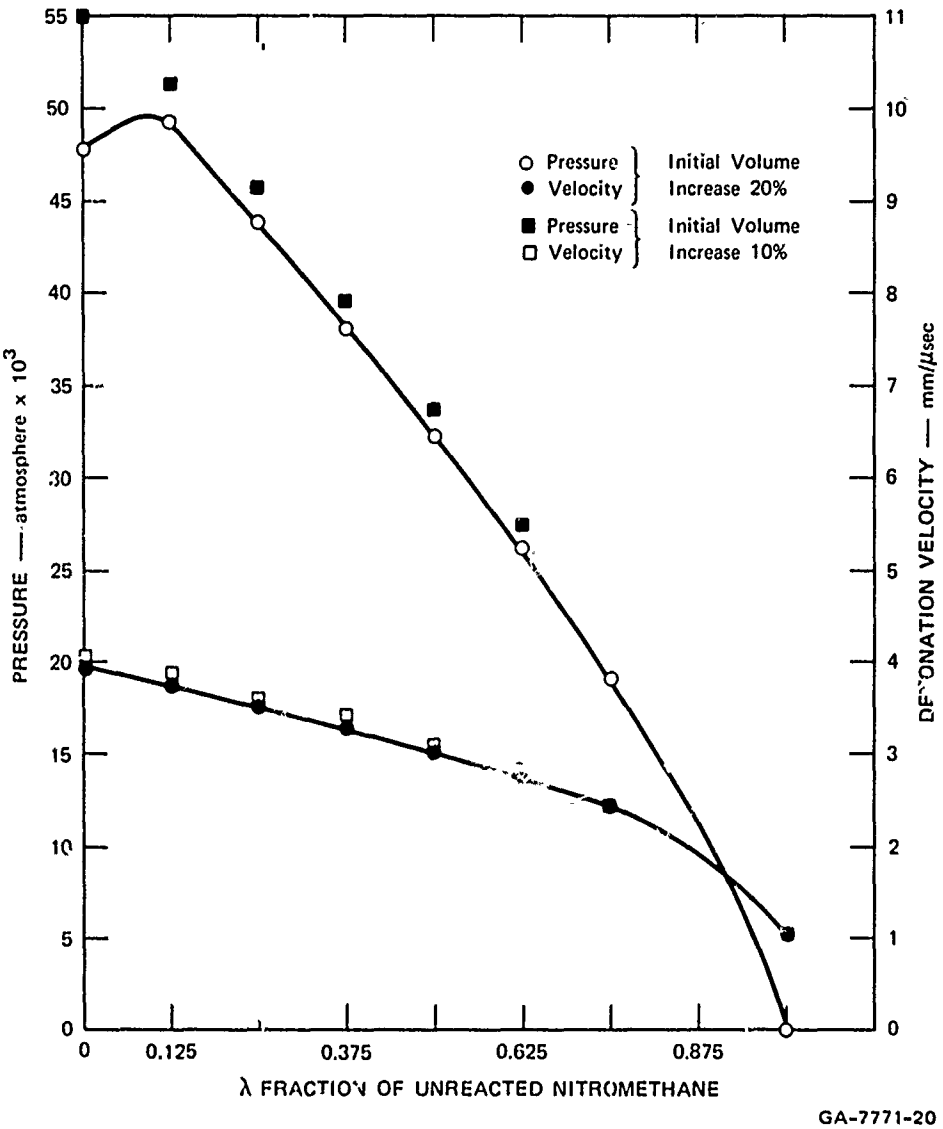

FIGURE B-3 DETONATION PARAMETERS VERSUS FRACTION OF UNREACTED NITROMETHANE

Appendix C

A "UNIVERSAL" HUGONIOT FOR LIQUIDS

A "UNIVERSAL" HUGONIOT FOR LIQUIDS*

R. W. Woolfolk, Michael Cowperthwaite, and Robert Shaw

Physical Sciences Division
Stanford Research Institute
Menlo Park, California 94025

*This work was supported by the U.S. Office of Naval Research under Contract No. N00014-70-C-0190 and by the U.S. Air Force Office of Scientific Research under Contract No. F44620-69-C-0079.

The universal Hugoniot curve[1-3] used previously to calculate shock temperature in liquid explosives[4,5] is not valid below 20 kilobars because it was constructed from shock wave data obtained at higher pressures. Moreover, it does not satisfy conditions defined in the initial state by the Rankine-Hugoniot jump conditions. The object of the present work was to extend the Hugoniot curve to the initial state and thus improve the thermodynamic description of liquids in the 1-bar to 20-kilobar region. The objective was attained by modifying the form of the Hugoniot curve to satisfy the initial conditions,[6] calibrating it with static pressure data for water,[7,8] and checking its validity with dynamic shock wave data for glycerine[9] and carbon tetrachloride.[10]

The Hugoniot curve defines the locus of shocked states obtainable from a given initial condition. It is obtained experimentally[11] from a determination of the states produced by constant velocity shocks propagating at different velocities. Experimental determination of a Hugoniot is usually very expensive and time-consuming, and requires considerable amounts of materials which are destroyed in the process. There is therefore a need for estimating Hugoniots from easily measured physical properties.

Following earlier work by Gibson and coworkers,[1] Woolfolk and Amster [2] and Voskoboinikov, Afanasenkov, and Bogomolov [3] have shown that the Hugoniots of liquids could be represented by a single normalized plot of the form

$$U/c_o = a_1 + (a_2 u/c_o) \qquad (1)$$

where U is the shock velocity, u is the particle velocity, c is the sound velocity, a_1 and a_2 are constants, and subscript zero denotes the initial

state at a pressure p of 1 bar. Eqn. (1) with $a_1 = 1.37$ and $a_2 = 1.62$ fitted[2] the experimental data which were in the range $u/c_o = 0.5$ to 2.5, corresponding to shock pressures in the range of 20 to 150 kbar.

The main problem with Eqn. (1) is that it does not satisfy the boundary condition $U = c_o$ at $u = 0$. Eqn. (1) therefore cannot be used in the region from 1 bar to 20 kbar. This low-pressure region is of interest because of its importance in low-velocity detonations.

Jacobs[6] has suggested that an additional term $(1-a_1)\exp[-a_3 u/c_o]$ with a_3 constant, be added to Eqn. (1) so that the boundary condition may be met. The form of the "universal" Hugoniot would then be

$$U/c_o = 1.37 - (0.37)\exp[-a_3 u/c_o] + 1.62\, u/c_o \qquad (2)$$

which reduces to $U/c_o = 1$ at $u = 0$. In Fig. 1 the experimental data are shown along with three calculated curves that correspond to $a_3 = \infty$, 5, and 1. Figure 1 indicates that the value of a_3 should be ≤ 5. An expression for a_3 was derived from thermodynamic identities relating the Hugoniot curve and the isentrope. The constant a_3 was evaluated using echo-sounding data for water.

The identity for the initial slope of the Hugoniot in the (U-u) plane

$$\left(\frac{dU}{du}\right)_{p=1} = \frac{v_o^3}{4c_o^2}\left(\frac{\partial^2 p}{\partial v^2}\right)_{s_o} \qquad (3)$$

where v denotes specific volume and s denotes specific entropy, and the thermodynamic identity for an isentrope

$$\left(\frac{\partial^2 p}{\partial v^2}\right)_s = \frac{2c}{v^2}\left[\frac{c}{v} - \left(\frac{\partial c}{\partial v}\right)_s\right] \tag{4}$$

were used to determine the constant a_3 in Eqn. (2). Differentiating Eqn. (2) with respect to u gives the slope of the Hugoniot as

$$dU/du = 1.62 + 0.37\ a_3 \exp(-a_3 u/c_o) \tag{5}$$

and the relationship between the initial slope of the Hugoniot and a_3 is obtained as

$$0.37\ a_3 = ((dU/du)_{p=1} - 1.62) \tag{6}$$

by setting u = 0 in Eqn. (5). The calculation of $(\partial^2 p/\partial v^2)_s$ at p = 1 bar with sound velocity data is then sufficient to evaluate a_3. The identity

$$\left(\frac{\partial c}{\partial v}\right)_s = \left(\frac{\partial c}{\partial v}\right)_p\left[1 + \frac{c^2}{v^2}\left(\frac{\partial v}{\partial p}\right)_c\right] \tag{7}$$

was used in the evaluation of a_3 because it is convenient to estimate the derivatives $(\partial c/\partial v)_p$ and $(\partial v/\partial p)_c$ with experimental data. Data from echo-sounding tables for pure water,[7] together with p-v-T data,[8] were used to construct a graph of the variation of sound speed with specific volume at pressures of 1, 50, 100, and 150 bar (see Figure 2). At p = 1 bar, T = 25°C, and c_o = 1493 m/sec, we estimate $(\partial c/\partial v)_{p=1}$ from the graph as

$$\left(\frac{\Delta c}{\Delta v}\right)_{p=1} = 1.027 \times 10^6\ \text{g/(sec cm}^2\text{)}$$

Similarly, from the graph, at constant c = 1493 m/sec, the following values of p and v were estimated:

p (bar)	v (cc/g)	Δv (cc/g)
1	1.00295	
		0.00325
50	0.99970	
		0.00290
100	0.99680	
		0.00275
150	0.99405	

Extrapolating to p = 1, we obtain

$$\left(\frac{\partial v}{\partial p}\right)_{c_o} = \left(\frac{\Delta v}{\Delta p}\right)_{c_o} = -7 \times 10^{-11} \text{ cm}^5/(\text{dyne g})$$

Substitution of $c_o = 1.493 \times 10^5$ cm/sec, v = 1.00295 cm^3/g, $(\partial v/\partial p)_{c_o} = -7 \times 10^{-11}$ cm^5/(dyne g), and $(\partial c/\partial v)_{p=1} = 1.027 \times 10^6$ g(sec cm^2) into Eqn. (7) gives $(\partial c/\partial v)_s = 5.66 \times 10^5$ g/(sec cm^2). Evaluating $(\partial^2 p/\partial v^2)_s = 2.12 \times 10^{11}$ sec^2/(g^3 cm^{-7}) with Eqn. (4) and $(dU/du)_{p=1} = 2.40$ with Eqn. (3) gives $a_3 = 2.1$ by substitution in Eqn. (5).

The region of Fig. 1 close to the origin has been replotted as Fig. 3, using Eqn. (2) and values of $a_3 = \infty$, 10, 5, 2, 1, and 0.1. Also plotted in Fig. 3 are experimental Hugoniot points for glycerin obtained by Erlich[9] and for carbon tetrachloride obtained by Lysne.[10] Until further data are available, we conclude that a value of $a_3 = 2$ is consistent with results of the calculations on water and with the experimental data on glycerin and carbon tetrachloride. In other words, Eqn. (2) becomes:

$$U/c_o = 1.37 - 0.37 \exp[-2u/c_o] + 1.62\, u/c_o \qquad (8)$$

It is concluded that the modified universal Hugoniot curve formulated in this note improves the thermodynamic description of liquids in the 1-bar to 20-kbar region.

Acknowledgments

We are greatly indebted to A. B. Amster of the U.S. Naval Ordnance Systems Command, who initiated this research and S. J. Jacobs of the U.S. Naval Ordnance Laboratory who suggested the form of the equation. We also thank D. F. Barnes of the U.S. Geological Survey for providing echo-sounding data, and D. C. Erlich for permission to quote his unpublished results on glycerin.

REFERENCES

1. F. C. Gibson, R. W. Watson, J. E. Hay, C. R. Summers, J. Ribovich, and F. H. Scott, "Sensitivity of Propellant Systems," Quarterly Report October 1 to December 1, 1964, U.S. Dept. of Interior, Bureau of Mines, Pittsburgh, Pennsylvania. Prepared for Bureau of Naval Weapons, Order 19-65-8023WEPS.

2. R. W. Woolfolk and A. B. Amster, Stanford Research Institute Project 4051, Technical Progress Report 67-2 (Semiannual), "Sensitivity Fundamentals," October 15, 1967.

3. I. M. Voskoboinikov, A. N. Afanasenkov, and V. M. Bogomolov, FGV (Phys. of Exp. and Comb.) No. 4 (1967) 585.

4. M. Cowperthwaite and R. Shaw, J. Chem. Phys. 53, (1970) 555.

5. R. Shaw, J. Chem. Phys. 54 (1971) 3657.

6. S. J. Jacobs, private communication, 1969.

7. D. J. Matthews, "Tables of the Velocity of Sound in Pure Water and Sea Water," Hydrographic Department, Admiralty, London, England, 1939.

8. N. E. Dorsey, "Properties of Ordinary Water-Substance," Reinhold Pub. Co., New York, 1940.

9. D. C. Ehrlich, unpublished work, SRI, 1971.

10. P. C. Lysne, J. Chem. Phys. 55 (1971) 5242.

11. J. M. Walsh and M. H. Rice, J. Chem. Phys. 26, (1957) 815.

74

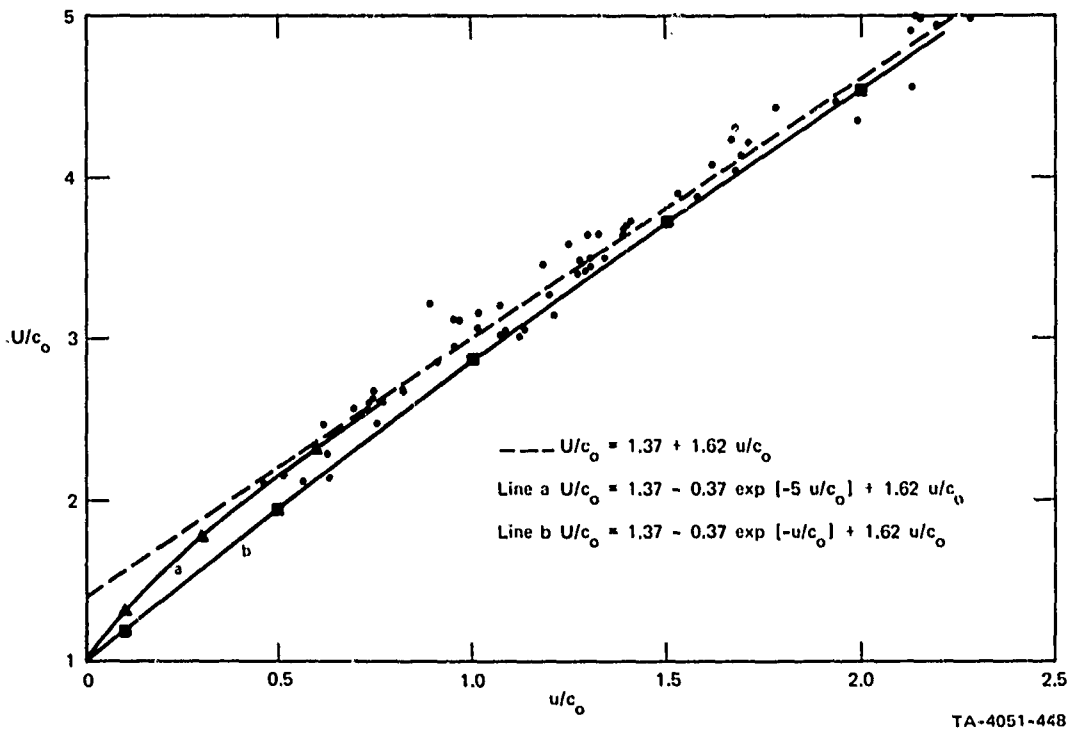

FIGURE C-1 NORMALIZED U-u PLOT

95

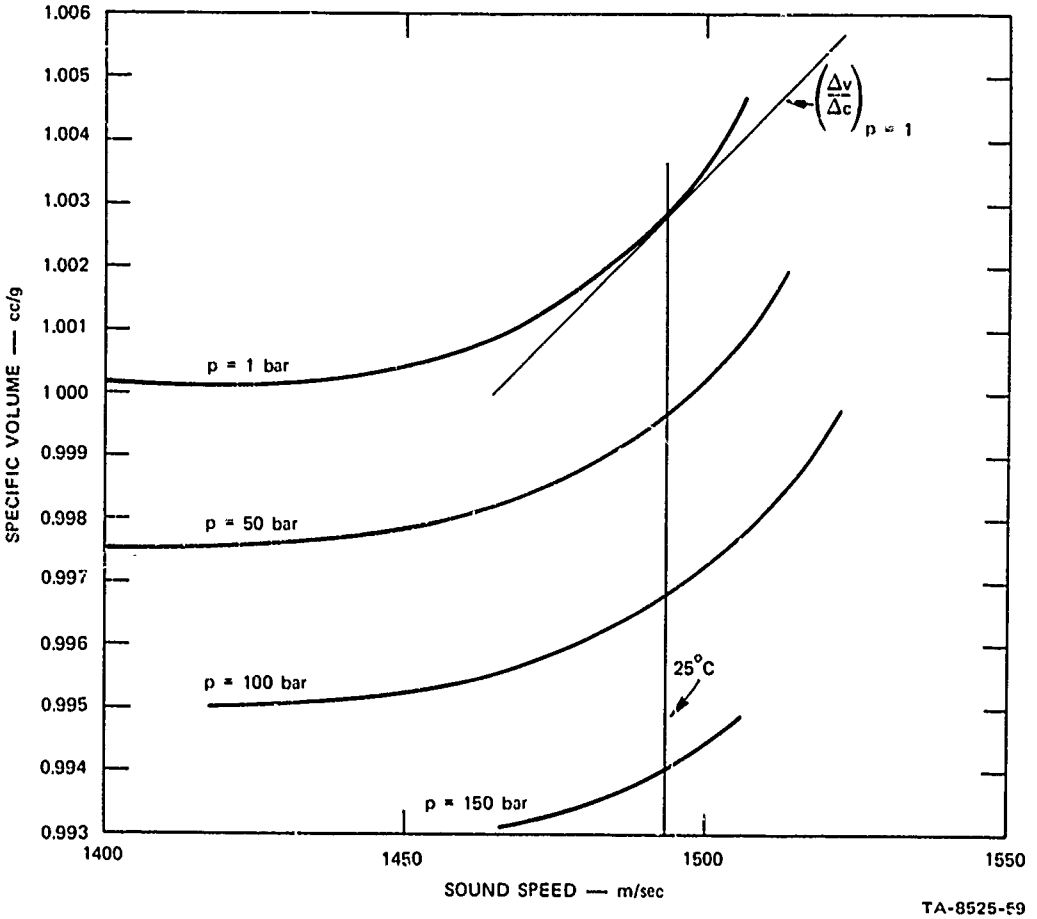

FIGURE C-2 SOUND SPEED IN PURE WATER AS A FUNCTION OF SPECIFIC VOLUME AT PRESSURES OF 1, 50, 100, AND 150 BAR

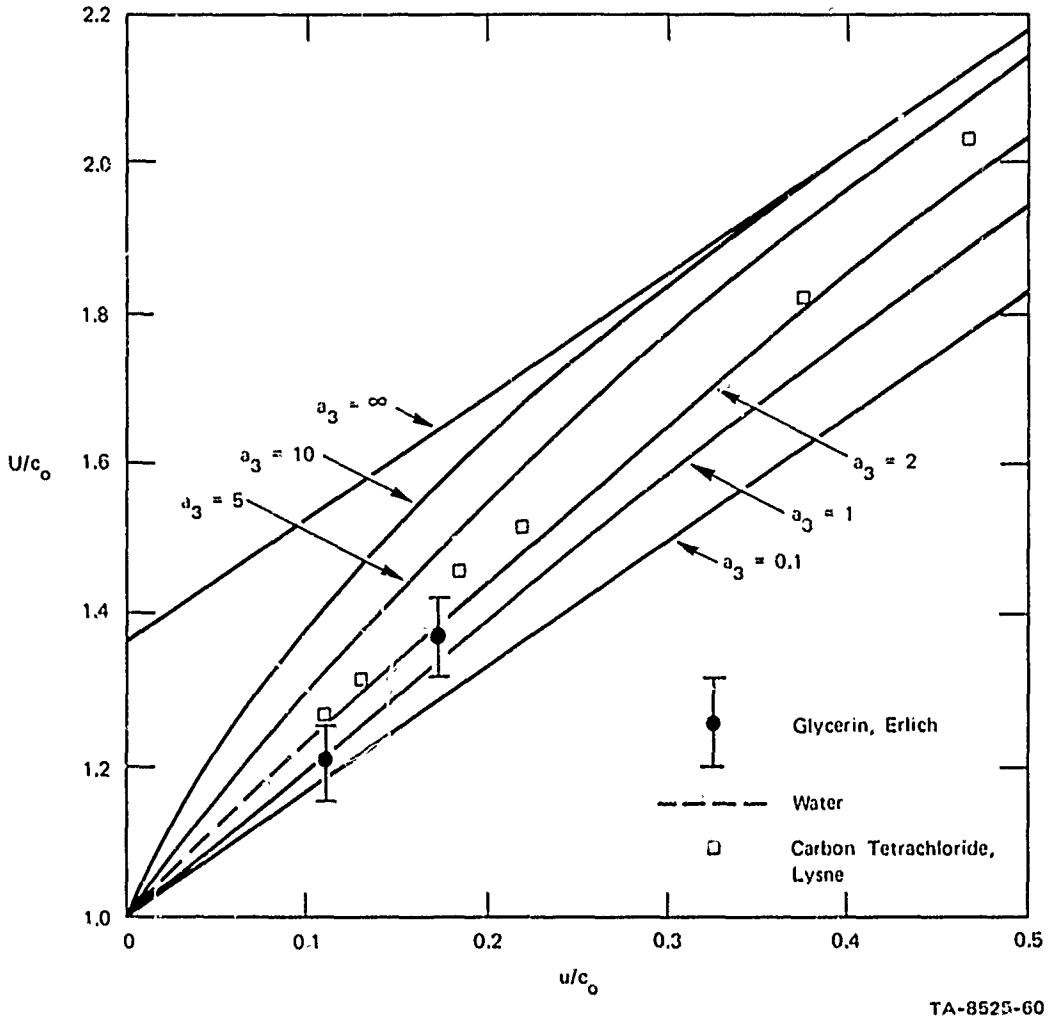

FIGURE C-3 CALCULATED NORMALIZED U-u PLOTS FOR VALUES OF a_3 = 0.1, 1, 2, 5, 10, AND ∞ IN THE EQUATION $U/c_o = 1.37 - 0.37 \exp[-a_3 u/c_o] + 1.62\ u/c_o$ SHOWING ERLICH'S EXPERIMENTAL GLYCERIN DATA, AND LYSNE'S EXPERIMENTAL CARBON TETRACHLORIDE DATA

Appendix D

COLLAPSE OF A VAPOR BUBBLE LEADING TO HOT-SPOT INITIATION

COLLAPSE OF A VAPOR BUBBLE*
LEADING TO HOT-SPOT INITIATION

By

David C. Wooten
Ultrasystems, Inc.
Newport Beach, California 92660

March 1972

* This work was supported by the U.S. Air Force Office of Scientific Research under Contract No. F44620-69-C-0079.

Introduction

The hot spots caused by adiabatic heating during the collapse of bubbles or cavities were proposed by Bowden and coworkers[1] in 1947 as a mechanism for the initiation of explosion in highly energetic liquids. This initiation mechanism was proposed to explain the high sensitivity of liquid or gelatinous explosives to mechanical impact. As a result of extensive subsequent investigations, the effect of hot spots on the shock sensitivity of liquid explosives is well understood. The early experiments by Yoffe[2] supported the view that initiation is due to compressive heating of entrapped gas or vapor spaces.

The detailed mechanism of hot-spot initiation by bubbles in some cases may be due to processes other than heating by adiabatic compression. For example, studies by Campbell et al.[3] show that initiation may take place by shock interactions caused by both solid inhomogeneities and bubbles. Mader,[4] in a two-dimensional numerical computation of the reactive flow around cylindrical and rectangular cross section rods or cavities placed parallel to the shock front, has given added support to the conclusions reached in these experiments. Heating sufficient to cause initiation by cylindrically symmetric shock interaction with a spherical bubble was also computed by Evans et al.[5] Hot-spot ignition caused by shock interaction or focusing at a bubble is of course increasingly effective with higher shock strengths. On the other hand, it is also conceivable that the Munroe jet effect could be responsible for bubble and cavity initiation at higher shock strengths. This mechanism was proposed by Bowden[6] and subsequently microjet ignition was observed experimentally by Watson and Gibson[7] and under different conditions by Bowden and McOnie.[8] At lower shock strengths, however, Gibson et al.[9] have shown that the velocity of the jet is not sufficient to cause shock initiation as the jet collides with the opposite side of the bubble.

80

Thus, hot-spot initiation by a bubble due to both shock focusing and microjetting are generally of interest for shock strengths in excess of about 50 kbar.

The important role of bubble hot-spot ignition in the initiation and propagation of low-velocity detonation (LVD), however, has recently stimulated renewed interest in hot-spot formation at lower shock overpressures in the 1 to 10 kbar range. The most plausible model of LVD is a cavitation model recently suggested by Watson et al.[10] and independently by Voskoboinikov et al.[11] In the cavitation model, precursor container wall waves cavitate the liquid ahead of a liquid shock; the cavitation bubbles are subsequently compressed by the liquid shock causing hot-spot-initiated reaction; and the resulting energy release in turn supports the liquid shock. This model has been further verified by Watson[12] who has photographed the cavitation ahead of the reaction zone and by Watson et al.[13] who more recently have reported tentative measurements of precursor wall waves capable of producing cavitation ahead of the reaction zone. In addition, the existence of individual burning sites rather than a continuous reaction front has been observed by Watson[12] in x-ray photographs of the LVD reaction wave, and Gibson et al.[14] have experimentally verified the dependence of bubble ignition on the strength of the initiating shock.

The cavitation model also explains the relatively long dark region observed between the shock front and the luminescent reaction zone.[12] Thus, the cavitation model, though it involves an incompletely understood interaction between the container and the liquid explosive, the formation of cavitation and subsequent hot-spot reaction, and as yet unknown criteria for stability, appears to offer the most plausible mechanism for the propagation of LVD.

Background

The dynamics of vapor bubbles has been a subject of extensive theoretical and experimental investigation for a number of years. In a sequence of early papers, Plesset and Zwick[15-17] calculated the rate of growth of vapor bubbles in slightly superheated steam under constant external pressure. Their calculations assume that the temperature variations in the liquid are appreciable only in a thin thermal boundary layer near the bubble wall. The predicted bubble radius R(t) is asymptotically proportional to $t^{\frac{1}{2}}$ when R is large enough so that surface tension is negligible, a result that was confirmed experimentally by Dergarabedian.[18] More recent work has extended the work of Plesset and Zwick[15-17] to more general cases.[19-21] Most of the work on the dynamics of vapor bubbles has been aimed, however, at boiling and related phenomena. Of more interest here is the collapse of a bubble leading to high interior temperatures causing local initiation of reaction which may ultimately ignite the bulk material leading to explosion.

Theoretical studies of hot-spot initiation that are related to the adiabatic compression of a bubble have been carried out by Zinn,[22] Enig,[23] and Gill.[24] These are computations of ignition delay time which are applicable to a bubble with a stationary radius and with no mass transfer at the bubble wall. In the present computations, however, we are interested in the temperature rise and the onset of reaction or ignition in a collapsing vapor bubble. We include here the effects of both heat and mass transfer (vaporization) at the bubble wall, and formulate the problem in Lagrangian coordinates that move with the bubble wall during collapse. It is assumed that both the vapor and liquid are nonviscous and, prior to collapse, they have the same temperature T_o. The interior of the vapor bubble is assumed to be uniform, an assumption that is justified provided that the thermal

diffusivity of the vapor is much greater than that of the liquid and that the speed of the bubble wall motion is much less than the sound speed in the vapor. The first condition is certainly true for most substances for, although the thermal conductivity of the liquid is about ten times greater than that of the vapor, the thermal diffusivity of the vapor is still much greater than that of the liquid. The second condition has been discussed by Hickling[25] in connection with the collapse of a bubble of inert gas in a liquid. Hickling found that the sound speed in the gas was indeed much higher than the velocity of the bubble wall for initial bubble radii of $R_o = 10^{-1} - 10^{-3}$ cm. and overpressures of about 4 atm. Under such conditions, the pressure in the vapor bubble remains approximately uniform because the effects of disturbances at the wall will have time to be propagated throughout the bubble interior. It is clear that during the early stages of collapse the assumption of uniform bubble interior will certainly be valid in the present calculation. Further, to keep the problem tractable, a spherical bubble will be assumed even though shock compression in general produces asymmetric collapse and, in addition, it is known that spherical bubbles are generally unstable during the latter stages of collapse.

Formulation of the Problem

A very general formulation of the equations governing the motion of a bubble in a liquid was given by Hsieh,[26] as well as simplified equations for a spherical bubble with a uniform interior. With the above assumptions and the additional assumptions that:

(1) No body force is present,
(2) There is no translational motion of the bubble relative to the liquid;
(3) Viscosity coefficients are zero throughout;
(4) The liquid is incompressible;
(5) The equation for the temperature in the liquid $T_\ell(r, t)$ can be written as

$$\frac{\partial T_\ell}{\partial t} + V_\ell \frac{\partial T_\ell}{\partial r} = \alpha_\ell \left(\frac{\partial^2 T_\ell}{\partial r^2} + \frac{2}{r} \frac{\partial T_\ell}{\partial r} \right) , \quad (1)$$

where r is the radial coordinate from the bubble center and α_ℓ is the thermal diffusivity of the liquid, which will be assumed constant. Since the liquid is treated as incompressible, and the density of the vapor ρ_v is generally much less than that of the liquid, from the continuity requirement the liquid velocity may be directly related to the bubble radius $R(t)$ as follows:

$$V_\ell = \frac{R^2 \dot{R}}{r^2} . \quad (2)$$

That is, the contribution of mass transfer (vaporization) at the bubble surface to R is neglected. Note that the assumption of uniform bubble interior requires that the quantities inside the bubble ρ_v, T_v, P_v are functions of time only. The initial condition will be that at $t = 0$ a bubble of radius R_o is at rest, with the vapor inside at initial

84

density and pressure of ρ_{vo}, P_{vo}, respectively. The assumption of uniform initial temperature T_o for the system requires that

$$T_v(0) = T_\ell(r,0) = T_o \quad . \tag{3}$$

Further, the boundary condition at the bubble wall requires that

$$T_v(t) = T_\ell(0,t) \tag{4}$$

and

$$\lambda_\ell \frac{\partial T_\ell}{\partial r}(0,t) = \frac{L}{4\pi R^2} \frac{d}{dt}\left(\frac{4}{3}\pi R^3 \rho_v\right) + \frac{\rho_v R C_v}{3} \frac{dT_v}{dt} + P_v \dot{R} +$$

$$+ \rho_v\left(\frac{4}{3}\pi R^3\right) QZ \exp\left[-E/\mathcal{R}T_v\right], \tag{5}$$

when L is the latent heat per unit mass, C_v is the specific heat at constant volume of the vapor, and λ_ℓ is the thermal conductivity of the liquid. The quantities λ_ℓ, L, and C_v are assumed constant, as are Q, Z, and E which denote, respectively, the specific heat of reaction, the frequency factor, and the activation energy. The last term in Eq. (5) is the heat release in the bubble due to gas phase reaction which is generally negligible until T_v reaches the order of $E/\mathcal{R}$.

Since the (uniform) temperature in the vapor bubble is determined by the temperature of the liquid at the bubble wall, it follows that the (uniform) pressure in the bubble P_v is given by the vapor pressure of the liquid at the wall or bubble temperature. We will therefore make the additional assumption that the vapor pressure is the bubble wall and that the bubble contains pure vapor. Thus, the possibility that

absorbed gas in the liquid may contribute to the interior pressure of the bubble is excluded, and the results will be applicable to a pure liquid or to cases in which the partial pressure of absorbed gases is negligible in comparison with the vapor pressure. The equilibrium vapor pressure requirement is certainly valid in the early stages of collapse until the rate of change of the pressure in the bubble becomes comparable to the kinetic rate of vaporization. To enable us to treat the problem analytically, we will relate the vapor pressure of the liquid, and hence the pressure in the bubble, to the temperature at the bubble surface by use of the Clasuis-Clapeyron equation

$$P_v = P_o \exp\left\{ \frac{L}{\Re T_o} \left(1 - \frac{T_o}{T_v} \right) \right\} , \qquad (6)$$

where $\Re$ is the ideal gas constant and P_o is the vapor pressure at the initial temperature T_o. Further, the thermodynamic quantities in the vapor phase will be related by the ideal gas equation of state

$$P_v = \Re \rho_v T_v . \qquad (7)$$

The additional equation required to complete the formulation of the problem is the differential equation for the motion of the bubble wall[26]

$$R \ddot{R} + \frac{3}{2} (\dot{R})^2 = - \frac{\left(P_\infty - P_v \right)}{\rho_\ell} , \quad t > 0 , \qquad (8)$$

where P_∞, assumed constant, is the initial pressure in the bulk liquid and corresponds to the pressure at large distance from the bubble during collapse. The initial conditions for Eq. (8) are taken as

$$R(0) = R_o \qquad (9)$$

and

$$\dot{R}(0) = 0 .$$

Equations (1), (2), (6), (7), and (8) now form a set for the dependent variables $V_\ell(r,t)$, $T_\ell(r,t)$, $P_v(t)$, $T_v(t)$, and $\rho_v(t)$, subject to the conditions of (3), (4), (5), and (9).

Introduce the dimensionless variables

$$
\begin{aligned}
x &= \frac{1}{3R_o^3}\left(r^3 - R^3(t)\right) \\
\hat{t} &= t/\tau_c \\
\hat{R} &= R(t)/R_o \\
\theta_v &= \frac{T_v - T_o}{T_o} \\
\theta_\ell &= \frac{T_\ell - T_o}{T_o}
\end{aligned}
\tag{10}
$$

and the parameters

$$
\begin{aligned}
\eta &= L/\Re T_o \\
\tau_c &= (P_\ell R_o^2/P_\infty)^{\frac{1}{2}} \\
\tau_h &= R_o^2/\alpha_\ell \\
\tau_r &= \Re T_o/QZ\ ,
\end{aligned}
\tag{11}
$$

where τ_c is the characteristic time for bubble collapse τ_h is the characteristic time for heat transfer to the bubble wall, and τ_r is the dimensionless frequency factor for the reaction term in Eq. (5).

Equation (1) can now be written as

$$\frac{\partial \theta_\ell}{\partial t} = \left(\frac{\tau_c}{\tau_h}\right) \hat{R}^4 \frac{\partial}{\partial x}\left[\left(1 + \frac{3x}{\hat{R}^3}\right)^{4/3} \frac{\partial \theta_\ell}{\partial x}\right] \qquad (12)$$

and the conditions (3), (4), and (5) become respectively;

$$\theta_v(0) = \theta_\ell(x,0) = 0 , \quad x \geq 0 \qquad (13)$$

$$\theta_v(\hat{t}) = \theta_\ell(0,\hat{t}) , \qquad \hat{t} \geq 0 \qquad (14)$$

and

$$\frac{\partial \theta_v}{\partial x}(0,\hat{t}) = (\gamma - 1) \frac{C_v}{C_\ell}\left(\frac{\rho v_o}{\rho_\ell}\right)\left(\frac{\tau_h}{Z_c}\right)\left(\frac{1}{\hat{R}^2}\right) \exp\left[\eta\left(\frac{\theta_v}{1+\theta_v}\right)\right] \times$$

$$\left\{\frac{d\hat{R}}{d\hat{t}}\left(\frac{\eta}{1+\theta_v} + 1\right) + \frac{\hat{R}}{3}\left(\frac{1}{1+\theta_v}\right) \frac{d\theta_v}{d\hat{t}}\left[\left(\frac{\eta}{1+\theta_v}\right)^2 - \frac{\eta}{1+\theta_v} + \frac{1}{\gamma-1}\right] + \right.$$

$$\left. + \frac{\hat{R}}{3}\left(\frac{1}{1+\theta_v}\right)\left(\frac{\tau_c}{\tau_r}\right) \exp\left[-\frac{E}{\Re T_o}\left(\frac{1}{1+\theta_v}\right)\right]\right\}, \qquad (15)$$

where γ is the ratio at specific heats of the vapor phase and ρ_{vo} is the initial density in the vapor phase.

The bubble equation (8) can be written as

$$\hat{R}\left(\frac{d^2\hat{R}}{dt^2}\right) + \frac{3}{2}\left(\frac{d\hat{R}}{d\hat{t}}\right)^2 = -\frac{P_\infty - P_v}{P_\infty} \qquad (16)$$

with the initial conditions

$$\hat{R}(0) = 1 \tag{17}$$

and

$$\frac{d\hat{R}}{d\hat{t}}(0) = 0 \quad . \tag{18}$$

Small-Time Solution

For small time defined by $\hat{t} \ll \tau_c$, the bubble radius has the form

$$\hat{R}^{(o)} = 1 + \hat{t}^2/2 \tag{19}$$

$$\text{so} \qquad \frac{d\hat{R}^{(o)}}{d\hat{t}} = \hat{t} \ . \tag{20}$$

Since $\vartheta_v(0) = 0$, the small-time expansion of $\vartheta_v(\hat{t})$ is $\ll 1$. A similar statement may be about about $\vartheta_\ell(x, \hat{t})$.

In general, for small time, since $\tau_h \ll \tau_c$ for situations of interest here, the temperature variation in the liquid occurs in a thin layer near the surface of the bubble such that in Eq. (12) we may neglect $x/\hat{R}^3$ relative to unity; that is $x/\hat{R} \tilde{=} x \ll 1$, an approximation that is discussed in detail in References 15 to 17 and 19. Thus Eq. (12) may be written for small time as

$$\frac{\partial \vartheta_\ell^{(o)}}{\partial \hat{t}} = \hat{\alpha} \ \frac{\partial^2 \vartheta_\ell^{(o)}}{\partial x^2} \ , \tag{21}$$

where $\hat{\alpha} = \tau_c/\tau_h$ and where Eq. (19) is used and only first-order terms are retained. Similarly, Eq. (15), to the first order is

$$\frac{\partial \vartheta_\ell^{(o)}}{\partial x}(0, \hat{t}) = (\gamma-1)\left(\frac{c_v}{c_\ell}\right)\left(\frac{\rho_{vo}}{\rho_\ell}\right)\left(\frac{\tau_h}{\tau_i}\right) \times$$

$$\left[- \hat{t}(\eta+1) + \frac{1}{3} \frac{d\eta_v^{(o)}}{d\hat{t}} \left(\eta^2 - \eta + \frac{1}{\gamma-1} \right) \right] \tag{22}$$

and the first-order parts of Eq. (13) and (14) are

$$\theta_\ell^{(o)}(x,0) = 0 \tag{23}$$

$$\theta_\ell^{(o)}(0,\hat{t}) = \theta_v^{(o)}(\hat{t}) \tag{24}$$

The reaction time is neglected since it is generally very small until θ_v becomes substantially greater than unity. Now write Eq. (22) in the form

$$\frac{\partial \theta_\ell^{(o)}}{\partial x}(0,\hat{t}) - A \frac{d\theta_v^{(o)}(\hat{t})}{d\hat{t}} = - B \hat{t} , \tag{25}$$

where

$$A = \beta/3 \left(\eta^2 - \eta + \frac{1}{\gamma - 1}\right) \tag{26}$$

$$B = \beta(\eta+1) \tag{27}$$

and

$$\beta = (\gamma-1)\left(\frac{C_v}{C_\ell}\right)\left(\frac{\rho_{vo}}{\rho_\ell}\right)\left(\frac{T_h}{T_c}\right) . \tag{28}$$

The problem consisting of the differential operation (21) with initial conditions (23) and boundary conditions (22) and (24) belongs to a class of problems solved by Carslaw and Jaeger[27] using Laplace transforms. The solution for small time is

$$\theta_\ell^{(o)}(x,\hat{t}) = \left(xA^3B\alpha^2\right) \left\{ \exp\left(\frac{x}{A\alpha} + \frac{\hat{t}}{A^2\hat{\alpha}}\right) \operatorname{erfc}\left[\frac{x}{2(\hat{\alpha}\hat{t})^{\frac{1}{2}}} + \frac{(\alpha\hat{t})^{\frac{1}{2}}}{A\hat{\alpha}}\right] - \sum_{n=o}^{\infty} \left[-2\frac{(\hat{\alpha}\hat{t})^{\frac{1}{2}}}{A\hat{\alpha}}\right]^n i^n \operatorname{erfc}\left(\frac{x}{2(\hat{\alpha}\hat{t})^{\frac{1}{2}}}\right) \right\} \tag{29}$$

Where i^nerfcy refers to the n^{th} integral of the erfcy function (see Reference 27). Consequently, the temperature at the bubble surface (x = 0) is

$$\theta_\ell^{(o)}(0,\hat{t}) = \theta_v^{(o)}(\hat{t}) = \left(\frac{\eta + 1}{\eta^2 - \eta + \frac{1}{\gamma-1}}\right)\left(\frac{3}{2}\hat{t}^{\,2}\right) . \qquad (30)$$

In comparison with the temperature in the bubble for an adiabatic collapse (no heat or mass transfer):

$$\frac{\theta_v^{(o)}}{\theta_{va}} = \left(\frac{\eta + 1}{\eta^2 - \eta + \frac{1}{\gamma-1}}\right)\left(\frac{1}{\gamma-1}\right) , \qquad (31)$$

where θ_{va} is the temperature for the adiabatic collapse of the same bubble. Generally η is in the range of 10-20 so the initial temperature rise in a collapsing vapor bubble with heat and mass transfer at the bubble wall may be almost an order of magnitude less than the corresponding rate of temperature rise for the adiabatic collapse of a similar bubble.

The temperature profile for small time is plotted in Figure 1 for a representative set of parameters.

References

1. F. P. Bowden, M. F. R. Mulcahy, R. G. Vines, and A. Yoffe, "The Detonation of Liquid Explosives by Gentle Impact: The Effect of Minute Gas Spaces," Proc. Roy. Soc. A.188, 291 (1947).

2. A. Yoffe, "Influence of Entrapped Gas on Initiation of Explosion in Liquids and Solids," Proc. Roy. Soc. A. 198, 737 (1949).

3. A. W. Campbell, W. C. Davis, and J. R. Travis, "Shock Initiation of Detonation in Liquid Explosives," Phys. Fluids, 4, 498 (1961).

4. C. L. Mader, "Initiation of Detonation by the Interaction of Shocks with Density Discontinuities," Phys. Fluids, 8, 1811 (1965).

5. M. W. Evans, F. H. Harlow, and B. D. Meizner, "Interaction of Shock or Rarefaction with a Bubble," Phys. Fluids, 5, 651 (1962).

6. F. P. Bowden, "The Initiation and Growth of Explosion in the Condensed Phase," 9th Symposium (International) on Combustion, Academic Press, N. Y. (1963), p. 499.

7. R. W. Watson, and F. C. Gibson, "Jets from Imploding Bubbles," Nature, 204, 1296 (1964).

8. F. P. Bowden, and M. P. McOnie, "Cavities and Micro Munro Jets in Liquids: Their Role in Explosion," Nature, 206, 380 (1965).

9. F. C. Gibson, R. W. Watson, J. E. Hay, C. R. Summers, J. Ribovich, and F. H. Scott, "Sensitivity of Propellant Systems," Bureau of Mines Quarterly Report, Bureau of Naval Weapons Order 19-66-8027-WEPS, January 1 to March 31, 1966.

10. R. W. Watson, C. R. Summers, F. C. Gibson, and R. W. Van Dolah, "Detonations in Liquid Explosives--The Low Velocity Regime, Proceedings, Fourth Symposium (International) on Detonation, Office of Naval Research, Dept. of the Navy, Washington, D.C., ACR-126; p. 117.

11. I. N. Voskoboinikov, A. V. Dubovik, and V. K. Bobolev, "Low Velocity Detonation in Nitroglycerine," Inst. Chem. Phys. Acad. Sci. USSR, Trans. from Dokl. Akad. Nauk, 161 (5), 1152 (1965).

12. R. W. Watson, "The Structure of Low-Velocity Detonation Waves," Twelfth Symposium (International) on Combustion, The Combustion Institute, Pittsburgh, (1969), p. 723.

13. R. W. Watson, J. Ribovich, J. E. Hay, and R. W. Van Dolah, "The Stability of Low-Velocity Detonation Waves," Fifth Symposium (International) on Detonation, ONR Report DR 163, (1970), p. 71.

14. F. C. Gibson, R. W. Watson, J. E. Hay, C. R. Summers, J. Ribovich, and F. H. Scott, "Sensitivity of Propellant Systems," Quarterly Report, U. S. Dept. of Interior, Bureau of Mines, Pittsburgh, February 2, 1966.

15. M. S. Plesset, and S. A. Zwick, "A Nonsteady Heat Diffusion Problem with Spherical Symmetry," J. Appl. Phys. 23, 95 (1952).

16. M. S. Plesset, and S. A. Zwick, "The Growth of Vapor Bubbles in Superheated Liquids," J. Appl. Phys. 25, 493 (1954).

17. M. S. Plesset, and S. A. Zwick, "On the Dynamics of Small Vapor Bubbles in Liquids," J. Math. Phys. 33, 308 (1955).

18. P. Dergarabedian, "Observations on Bubble Growths in Various Super-Heated Liquids," J. Fluid Mech. 9, 39 (1960).

19. G. Birkhoff, R. S. Margulies, and W. A. Horning, "Spherical Bubble Growth," Phys. Fluids, 1, 201 (1958).

20. S. A. Zwick, "Growth of Vapor Bubbles in a Rapidly Heated Liquid," Phys. Fluids, 3,685 (1960).

21. D. C. Gibson, "The Kinetic and Thermal Expansion of Vapor Bubbles," ASME Paper No. 71-FE-13, presented at Fluids Engineering Conference, Pittsburgh, May 9-12, 1971.

22. J. Zinn, "Initiation of Explosions by Hot Spots," J. Chem. Phys., 36, 1949 (1962).

23. J. W. Enig, "Approximate Solutions in the Theory of Thermal Explosions for Semi-Infinite Explosives," Proc. Roy. Soc. A. 305, 205 (1968).

24. S. P. Gill, "Initiation and Decomposition of Nitromethane at 10-kbar Pressure," Physics International Technical Report-70-2, March 1970.

25. R. Hickling, "Effects of Thermal Conduction in Sonoluminescence," J. Acoust. Soc. Am., 35, 967 (1963).

26. D. Y. Hsieh, "Some Analytical Aspects of Bubble Dynamics," J. Basic Eng., 87, 991 (1965).

27. H. S. Carslaw, and J. C. Jaeger, Conduction of Heat in Solids, Second Ed., Oxford University Press, London (1959).

95

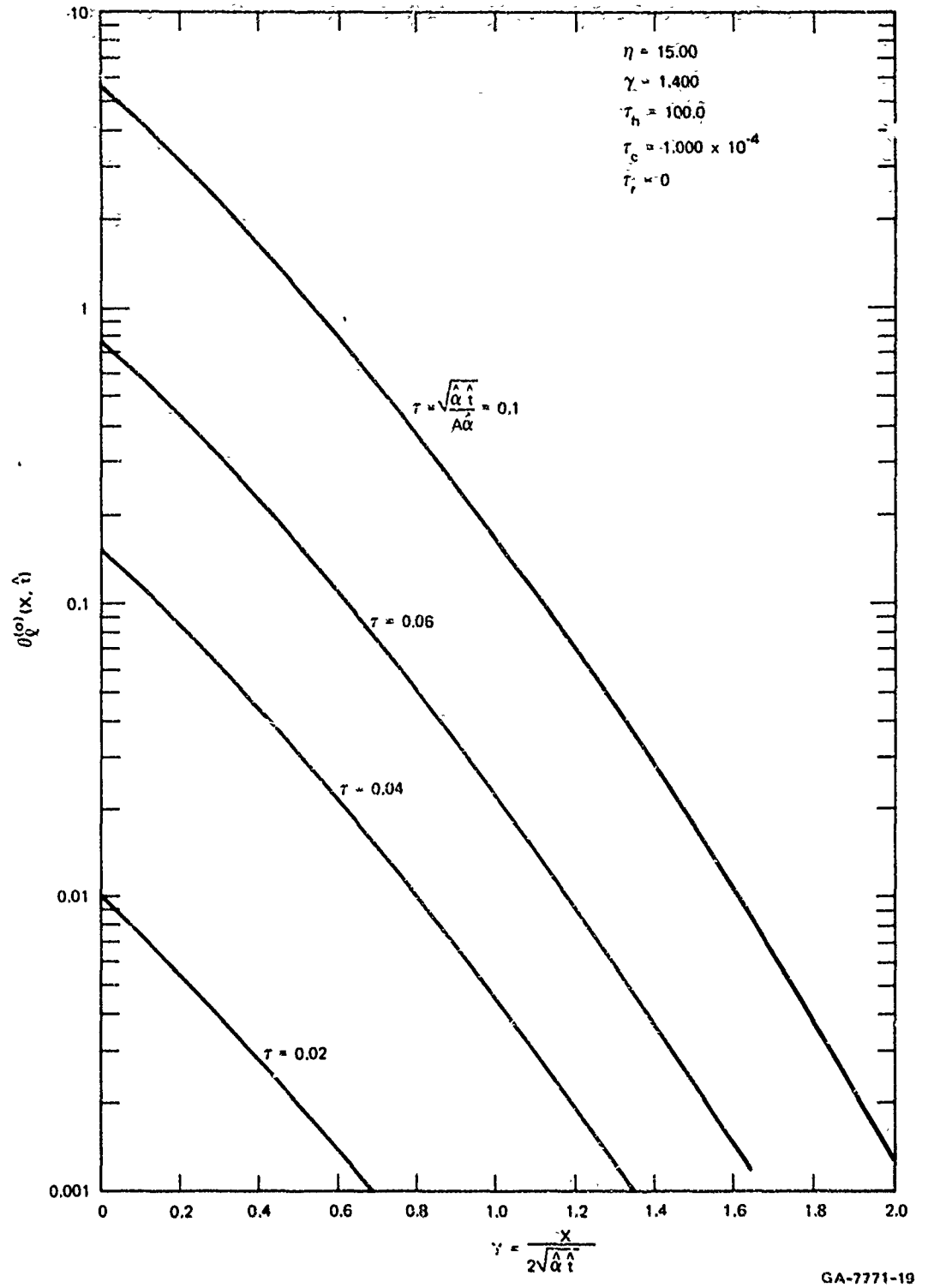

FIGURE D-1 TEMPERATURE PROFILES IN LIQUID FOR SMALL-TIME SOLUTION (EQ. 29)

Appendix E

MEASUREMENT OF PRESSURF IN LOW-VELOCITY DETONATION

MEASUREMENT OF PRESSURE IN LOW-VELOCITY DETONATION*

By

David C. Erlich
Stanford Research Institute
Menlo Park, California 94025

May 1972

* This work was supported by the U.S. Air Force Office of Scientific Research under Contract No. F44620-69-C-0079.

ABSTRACT

A pair of piezoresistant ytterbium stress gages were used to record pressure-time histories in liquid monopropellants in a study of the shock initiation of low velocity detonation (LVD). The propellant was contained in a cylindrical steel tube, and the initiating shock was produced by a tetryl pellet-attenuator donor system. Variation of the propellant, the wall thickness-to-diameter ratio of the tubes, and the initial shock pressure from 30 to 50 kbars resulted in (a) shock decay with no appreciable reaction, (b) initiation of LVD, and (c) initiation of high velocity detonation (HVD). Peak pressures recorded at 4 to 10 inches down the tube were in the 1- to 2-kbar range for shock decay, and in the 4- to 7-kbar range for LVD, but no pressures were recorded for HVD. The average LVD propagation velocity measured with the gages was about 2.0 mm/μsec for ethyl nitrate and about 3.0 mm/μsec for FEFO.

Introduction

This paper presents an experimental investigation of the shock initiation of low velocity detonation (LVD) in liquid monopropellants contained in cylindrical steel tubes. The object of the work was to achieve a more quantitative description of LVD. Since LVD propagation velocities had been measured in previous studies,[1,2] and the circumferential strain histories had also been examined,[3] a better description of states attained in the liquid was required to achieve this objective. Piezoresistant in-material ytterbium stress gages were therefore used in the experiments to measure the pressure time histories of liquid monopropellant during the initiation and propagation of LVD. A pair of gages were used in each experiment so that the pressure records could be used to determine propagation velocities.

Experimental Procedure

Figure 1 is a schematic diagram of the LVD experiments that were performed in the Stanford Research Institute explosives vault facility. A cylindrical seamless cold-rolled steel tube was used to contain the liquid. To the bottom of the tube was attached a 3-inch diameter disk of Homalite,* two 2-inch diameter by 1 inch thick pellets of tetryl, and one 1/4-inch thick by 1/2-inch diameter tetryl pellet. The tetryl detonation was initiated by an exploding bridgewire detonator in contact with the small pellet. The Homalite disk served as a stress pulse attenuator and its thickness was chosen to produce the desired peak pressure in the liquid. To determine this pressure, a standard four-terminal piezoresistant manganin stress gage was placed in the Homalite 1/32 of an inch from the surface in several of the experiments to record the peak stress that propagates into the liquid.

Two π-shaped 4-terminal piezoresistant ytterbium stress gages, photoetched from 0.001-inch thick foil, were mounted on a long strip of 0.003-inch-weave fiberglass cloth whose width was the same as the inside diameter of the tube. Long thin copper leads were soldered onto the gage terminals and a layer of Homalite was spread over the fiberglass to contain the gages and leads in a stiff 0.007-inch thick package. Fiberglass fins to ensure that the gage package remained in the center of the tube were attached and the package was slid into the tube and glued into place with the leads emerging from the top.

This arrangement of the gage package was motivated by several factors. First of all, since the package had a very small cross section in the plane of the expected shock front (perpendicular to the tube axis), it wouldn't move much as the shock and/or detonation wave forced the liquid to move up the tube. Second, any motion of the

* Trade name, Homalite Corporation.

gage package would not stretch and break the leads as quickly as if the leads had been attached to the tube wall. And third, since the coupling of the liquid and tube wall shock responses is very critical to the LVD phenomenon, it was desirable to avoid interference with the integrity of the wall, as would have occurred had the leads needed to emerge from the walls. One disadvantage of this orientation of the gage was an increase in the response time of the gage. Since the thickness of the active element in the direction of shock propagation was about 0.020 inch, the fastest rise that could be seen by the gage was about 250 nsec.

For several experiments, one or two Micro-Measurements Type EA-06-5006B-120* strain gages were glued to the outside of the tube wall adjacent to the location of the stress gages on the inside of the tube. They were oriented to measure hoop or circumferential strain and thus to compare the strain histories in these and earlier experiments,[4] and possibly to determine the time lag between LVD initiation at the center of the tube and the circumferential expansion of the tube.

Eight experiments were performed as part of the LVD program. The relevant experimental parameter for each of the shots is given in the upper half of Table 1. For the first 5 shots, ethyl nitrate was used for the liquid monopropellant and wall thickness-to-diameter ratios and attenuator thicknesses were chosen that had previously been successful in LVD initiation in similar materials.[3,4] When it became clear that it was difficult to create a steady-state LVD wave in ethyl nitrate (see next section), it was decided to switch to FEFO (fluorodinitro-ethylformal), a liquid known to be more sensitive to LVD initiation.[5] After shot No. 6 failed to cause detonation in the FEFO, the liquid was analyzed and was shown to contain a considerable amount of impurities. A new batch of FEFO was prepared for shot Nos. 7 and 8.

---

* Micro-Measurements, Romulus, Michigan.

All of the shots were instrumented except for shot No. 2, whose purpose was simply to determine by terminal observation if LVD had taken place. For all of the instrumented shots, a pulsed constant-current power supply was used in conjunction with the ytterbium and manganin stress gages and the signals were recorded on oscillographs in the manner described by Keough.[6] The piezoresistance coefficient of ytterbium (the factor relating change in gage resistance to stress) used in that data analysis was that determined by Ginsberg.[7]

Experimental Results

The results of the LVD experiments are tabulated in the bottom half of Table 1. Terminal observations of the remains of the steel tube were made to determine what type of detonation, if any, the liquid underwent. Figure 2 contains photographs of the tube remains for the three different outcomes that were observed, as well as a photograph of the tube prior to detonation. For the case in which no liquid detonation took place, the tube is undamaged except for the first inch or two adjacent to the explosive pellet. For the case in which the liquid underwent LVD, the section of tube below the liquid level broke into several pieces which were often severely bent or twisted. Some of these pieces did not break off from the undamaged upper section of the tube (the section above the liquid line) but bent back beyond the undamaged section in the shape of a partially peeled banana (with the fruit removed). This was particularly true of the ethyl nitrate shots No. 3, 4, or 5, where analysis of the gage records indicated a nonsteady state LVD, as will be discussed shortly. For the case in which the liquid underwent HVD, the tube broke into many long very thin fragments, as would be expected due to the very high pressures in the tube during an HVD. For shot No. 7 in which HVD occurred, no stress records were obtained due primarily to high propagation velocity of the HVD wave (between 6 and 7 mm/μsec), which caused the wave to pass the ytterbium gage location long before the triggering of the gage power supplies and oscilloscopes, which had been set to expect a slower velocity LVD wave.

The peak pressures recorded by the various stress gages are also given in Table 1 and the average propagation velocity of the peak stress seen by the ytterbium gages for the shots in which both gages produced analyzable records. A typical manganin gage record, that from shot No. 1, is shown in Figure 3. There is an initial peak of ~59 kbar which is

the stress that first reaches the gage plane in the Homalite, followed by a drop to ≈ 46 kbar, which is the stress induced into the liquid, and is lower due to the impedance mismatch between the Homalite and the liquid. Since the attenuator thickness was nearly the same for shots Nos. 1-5, and since the explosive pellet configuration was identical for all of the shots, it can be assumed that very nearly the same stress was induced into the ethyl nitrate for shots Nos. 1-5. Manganin gage records for the shots using FEFO yielded a pressure of ≈ 43 kbar for shots Nos. 6 and 7 using approximately a 1-inch thick attenuator, and ≈ 33 kbar for shot No. 8, which used a 1½-inch thick attenuator.

The ytterbium gages generally worked very well in measuring the liquid pressure histories for the shots in which the liquid underwent LVD. A couple of the ytterbium records (those from shot No. 8) exhibited a significant amount of high-frequency noise, but the remainder of the records had excellent signal-to-noise ratios. The records from the two ytterbium gages in shots Nos. 3 and 5 are shown in Figures 4 and 5, respectively. Observation of the various records from shots Nos. 3, 4, and 5, however, showed that the pressure histories at the two locations are qualitatively dissimilar for each shot. This is most clearly seen in Figure 4. The first gage, located at a distance of 6 inches from the detonating end of the tube, recorded a rapid rise (less than 1 μsec) to a peak pressure of about 2½ kbar and then a slow decay to zero pressure. Furthermore, the gage remained continuous for at least 20 μsec following the initial rise. On the other hand, the second gage, located at 10 inches from the end of the tube, exhibited a slower rise (more than 3 μsec) to a stress of over 5 kbar and then a nearly level plateau until the gage began to stretch and break 3 μsec later. The latter gage record is more like that to be expected in an LVD, while the lower stress and longevity of the former is indicative of no LVD in the immediate vicinity of the gage package. The records

from shot No. 5 exhibit similar tendencies, as shown in Figure 5, except that here the gage, located 4½ inches from the end of the tube, has a higher peak pressure (4.1 kbar) and shorter recording life than the gage located 7½ inches from the ends (with a peak pressure of 2.7 kbar). Since previous experimental studies and computer simulation indicate that LVD should start at distances of less than a few inside diameters down the tube, it is reasonable to assume that if a steady-state LVD were to be initiated in the tube, it would begin before the pressure pulse reaches the first gage location. Therefore it appears that a steady-state LVD wave was not produced in the region between the two ytterbium gages. More likely a pulsating or oscillatory LVD was produced, or perhaps merely a few isolated hot spots were initiated at various points in the tube. The higher pressure seen by one of the gages in both shot No. 3 and No. 5 as compared to shot No. 4, the higher peak pressure propagation velocity (about 2.00 mm/μsec as compared to 1.55 mm/μsec), and the fact that the tube in shot No. 4 was less damaged than the tube in shots 3 and 5 indicate that significantly less of the liquid in shot No. 4 underwent LVD than in shots No. 3 or No. 5.

Many explanations are possible for the failure to initiate a steady-state LVD in ethyl nitrate. Insufficient experimental data are available to predict precisely the conditions under which such a phenomenon will occur. It is therefore very possible that the experimental parameters chosen, such as the wall thickness-to-tube diameter ratio and attenuator thickness, were slightly different from those needed to achieve steady-state LVD. Perhaps ethyl nitrate is sufficiently insensitive in the region of these parameters.

The two stress gage histories for shot No. 8 using FEFO as the liquid were much more qualitatively alike, although high frequency noise obscured their structure somewhat. Furthermore the higher

measured peak pressures (4 to 7 kbar) and faster average propagation velocity (3 mm/μsec), despite the liquid being hit by a lower stress, indicated that a steady-state LVD was more likely initiated in FEFO than in the ethyl nitrate.

The final experimental result to be reported was that of the strain recorded for shot No. 4 (the strain gage records in shot No. 1 were too noisy to analyze). The peak circumferential strain seen at the distance of 10 inches from the end of the tube was 0.2%. Comparison with the computer simulation reported in Appendix A indicated that a 0.2% strain corresponds to an internal liquid pressure of a few kilobars, which is just that recorded by the stress gage. Furthermore LVD would produce a circumferential strain in the tube wall of more than 1% shortly after the wave passed that section of the tube. This is yet another indication of the absence of LVD in the region 10 inches from the detonated end of the tube for shot No. 4.

Conclusions

Although peak pressure measurements have been reported[4] the results reported here are the first direct measurements of pressure history in a liquid undergoing LVD. In the shots in which successful LVD was initiated, peak pressures of about 4 to 7 kbar were observed which is consistent with other observations of LVD.[1-4] The measurements were taken with a minimum of interference with the detonation wave by the use of very small gages. Therefore, the rise times and pressure history measured by the gages are believed to be closely representative of the true stress histories in an LVD wave. This technique should prove useful for recording pressure history ahead of and within LVD waves for comparison with theoretical prediction and to gain a better understanding of LVD behavior in various liquids as a function of confinement, initiating shock strength, and other experimental parameters.

Acknowledgment

The author wishes to thank Dr. R. W. Woolfolk for preparing the liquid samples and for many helpful discussions concerning the initiation of low-velocity detonation.

References

1. R. W. Woolfolk, and A. B. Amster, "Low Velocity Detonations: Some Experimental Studies and Their Interpretation," Twelfth Symposium (International) on Combustion, The Combustion Institute, Pittsburgh (1969) p. 731.

2. R. W. Watson, C. R. Summers, F. C. Gibson, and R. W. Van Dolah, "Detonations in Liquid Explosives--The Low Velocity Regime," Proceedings, Fourth Symposium (International) on Detonation, ACR-126, Office of Naval Research, Dept. of the Navy, Washington, D.C., p. 117.

3. R. W. Watson, J. Ribovich, J. E. Hay, and R. W. Van Dolah, "The Stability of Low-Velocity Detonation Waves," Fifth Symposium (International) on Detonation, ONR Report DR 163, (1970) p. 71.

4. D. C. Wooten, H. R. Bredfeldt, R. W. Woolfolk, and R. J. Kier, "Investigations of Low-Velocity Detonation Phenomena in Liquid Propellants, Fuels, and Explosives," Annual Report, AFOSR Scientific Report AFOSR 70-1005TR, March 1970.

5. R. W. Woolfolk, Private Communication.

6. D. D. Keough, "Development of High Sensitivity Piezoresistive Shock Transducer for the Low Kilobar Range," Final Report, Stanford Research Institute Project No. PGU 6979, (1968) (unpublished).

7. M. D. Ginsberg, "Calibration and Characterization of Ytterbium Stress Transducer," Final Report, Stanford Research Institute Project No. 7511 (1971) (unpublished).

Table 1

LVD EXPERIMENTS: PARAMETERS AND DATA

Shot No.	1	2	3	4	5	6	7	8
Liquid Used	Ethyl nitrate	Ethyl nitrate	Ethyl nitrate	Ethyl nitrate	Ethyl nitrate	FEFO*	FEFO	FEFO
Pipe I.D. (in.)	1.00	1.00	1.00	1.00	0.75	0.75	0.75	0.75
Pipe Wall Thickness (in.)	0.25	0.125	0.125	0.125	0.125	0.125	0.125	0.125
Pipe Length (in.)	24	12	24	24	18	18	18	18
Height of Liquid in Tube (in.)	18	12	18	18	14	14	14	14
Thickness of Homalite Attenuator (in.)	1-1/32	1	1	1	1	1-1/32	1	1-17/32
Gages Used:								
1. Manganin Gage in Homalite	Yes	-	-	-	-	Yes	-	Yes
2. Ytterbium Gage 1 - distance down pipe (in.)	6	-	6	6	4½	4½	4½	4½
3. Ytterbium Gage 2 - distance down pipe (in.)	10	-	10	10	7½	7½	7½	7½
4. Strain Gage 1 - distance (in.)	6	-	-	-	-	-	-	-
5. Strain Gage 2 - distance (in.)	10	-	-	10	-	-	-	-
Shot Results:								
Type of Detonation Initiated†	None	LVD	LVD	LVD	LVD	None	HVD	LVD
Peak Liquid Pressures Measured:								
by Manganin Gage (kbar)	46	-	-	-	-	43	-	33
by Ytterbium Gage 1 (kbar)	‡	-	2.5	2.65	4.1	‡	‡	7.3
by Ytterbium Gage 2 (kbar)	1.8	-	5.2	2.4	2.7	1.3	‡	4.0
Propagation Velocity of Peak Pressure seen by Yt gages (mm/μsec)	‡	-	2.05	1.55	1.97	‡	‡	2.97
Peak Strain seen by Strain Gage 2	‡	-	-	0.2%	-	-	-	-

* Subsequent analysis of this FEFO batch showed that it contained a considerable amount of impurities.

† As determined by terminal observation.

‡ Data not analyzable.

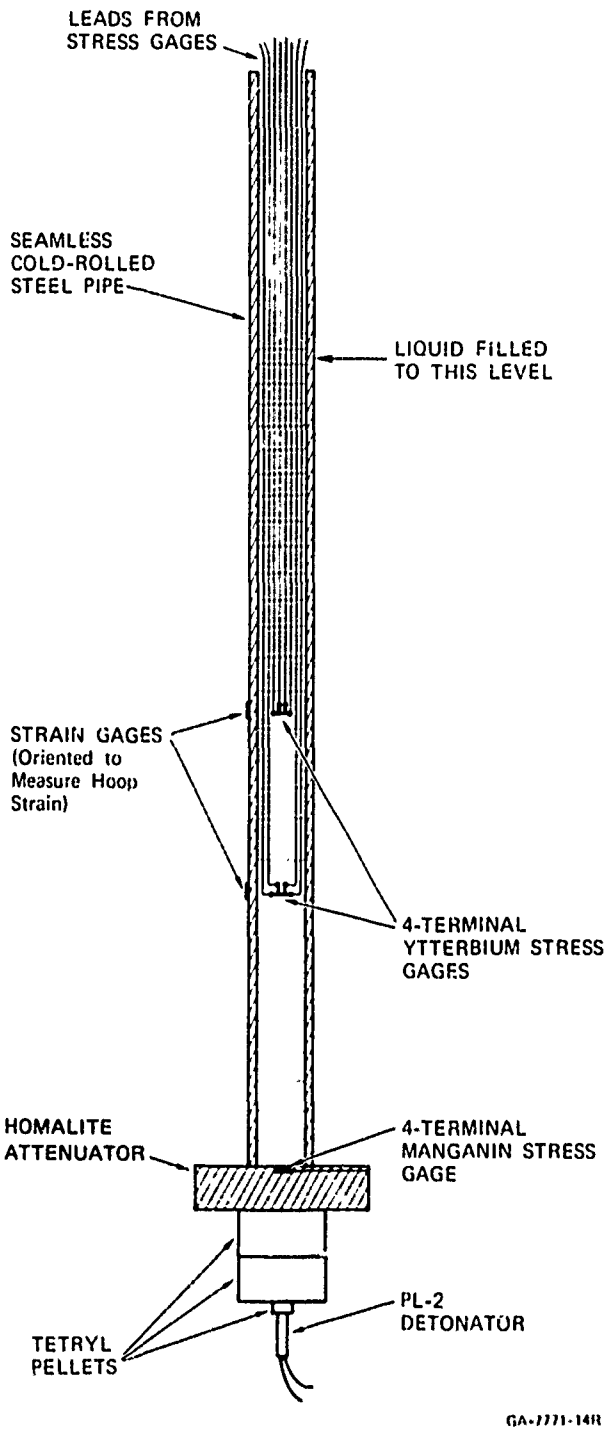

FIGURE E-1 SCHEMATIC DIAGRAM OF LVD EXPERIMENTS

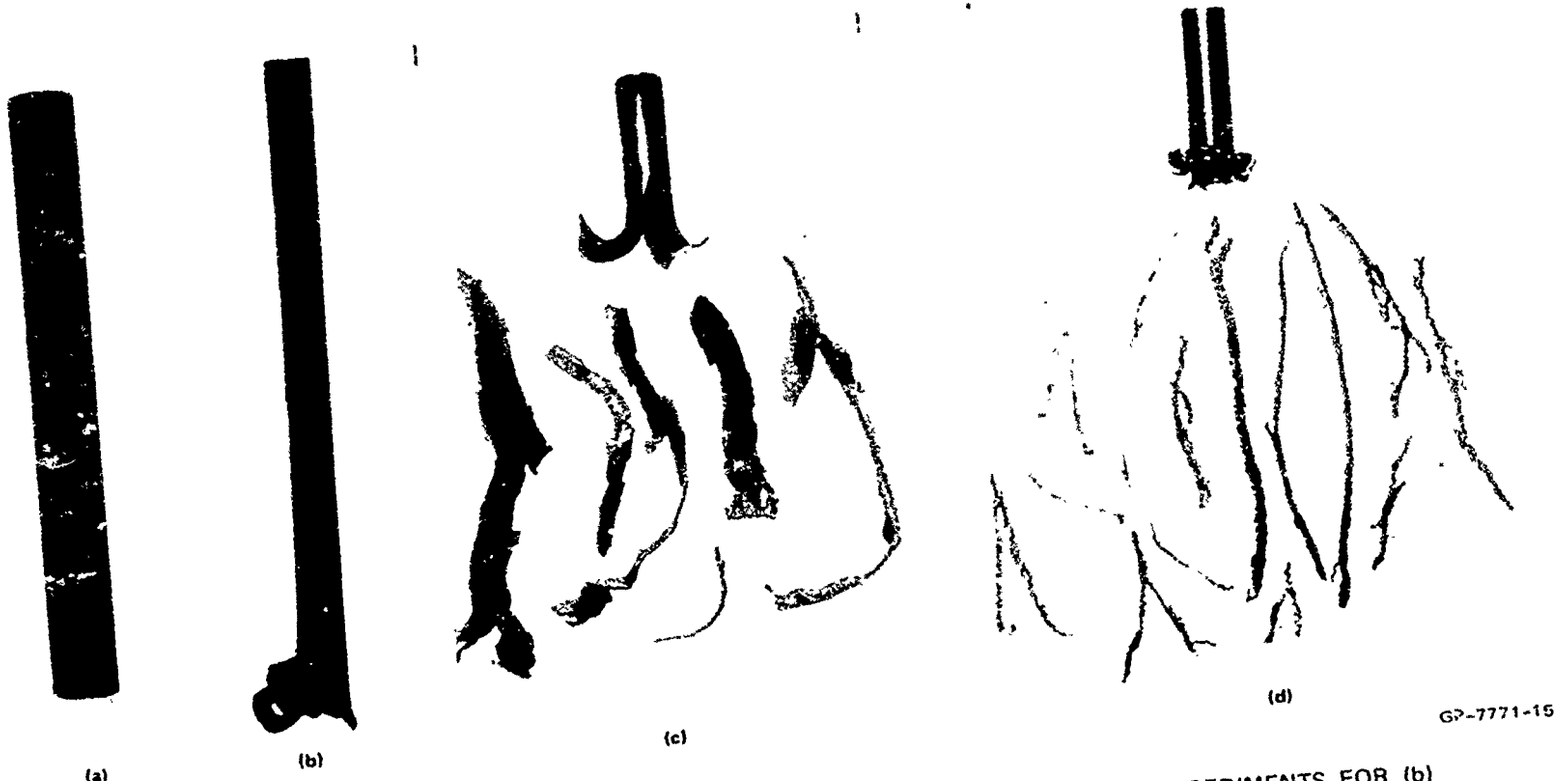

FIGURE E-2 PHOTOGRAPH OF STEEL TUBES AND FRAGMENTS RECOVERED FROM LVD EXPERIMENTS FOR (b) SHOT NO. 6, IN WHICH NO LIQUID DETONATION OCCURRED, (c) SHOT NO. 8, IN WHICH LOW VELOCITY DETONATION OCCURRED, AND (d) SHOT NO. 7 IN WHICH HIGH VELOCITY DETONATION OCCURRED; AS WELL AS (a) STEEL TUBE AND HOMALITE ATTENUATOR PRIOR TO DETONATION

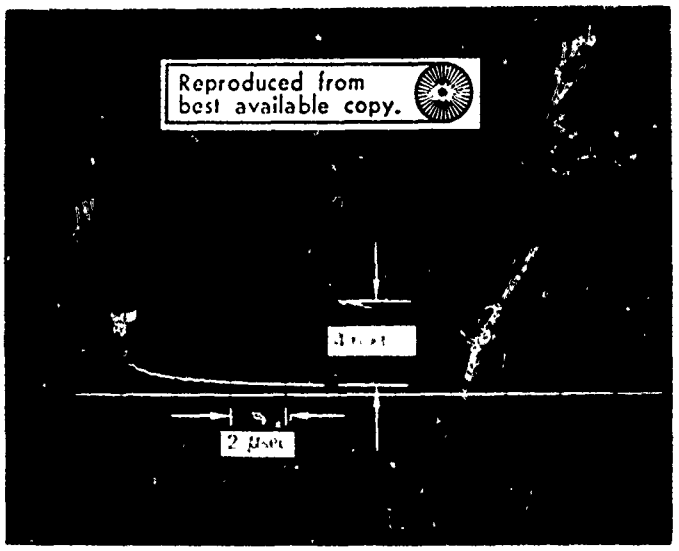

GP 7771 16

FIGURE E-3 OSCILLOGRAM FROM MANGANIN STRESS GAGE IN SHOT NO 1

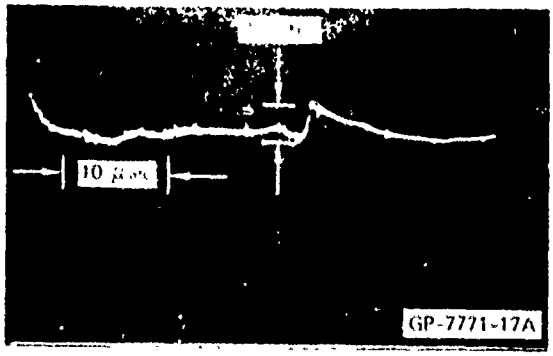

(a) 6 inches DOWN THE TUBE

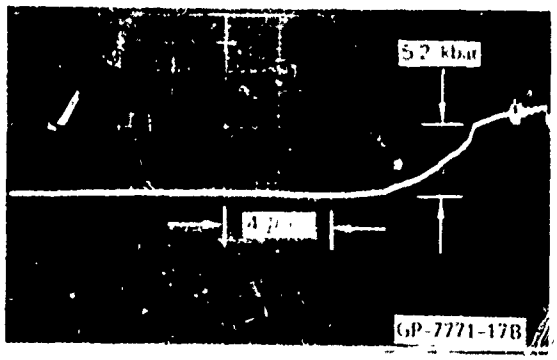

(b) 10 inches DOWN THE TUBE

GP 7771 17

FIGURE E-4 OSCILLOGRAMS FROM SHOT NO 3 FOR THE YTTERBIUM STRESS GAGES AT DISTANCES SHOWN IN (a) AND (b)

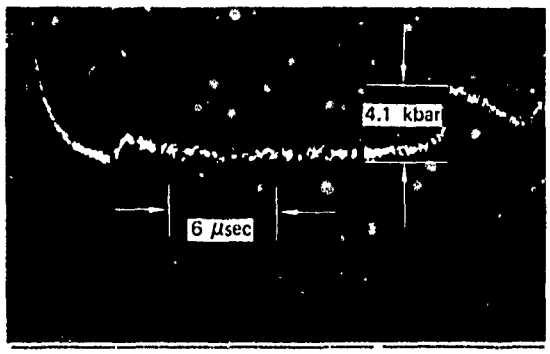

(a) 4-1/2 inches DOWN THE TUBE

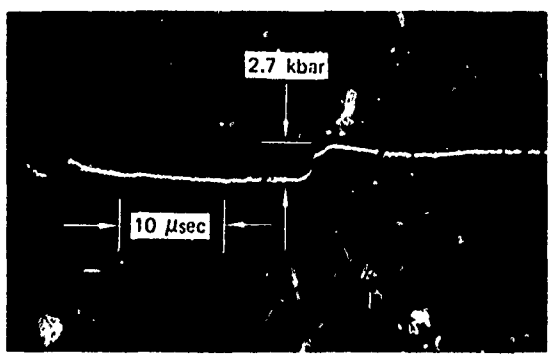

(b) 6 inches DOWN THE TUBE

GP 7771-18

FIGURE E-5 OSCILLOGRAMS FROM SHOT NO. 5 FOR THE YTTERBIUM STRESS GAGES AT DISTANCES SHOWN IN (a) AND (b)